Werk

Jahr: 1983
Kollektion: fid.geo
Signatur: 8 Z NAT 2148:52
Digitalisiert: Niedersächsische Staats- und Universitätsbibliothek Göttingen
Werk Id: PPN1015067948_0052
PURL: http://resolver.sub.uni-goettingen.de/purl?PPN1015067948_0052

LOG Id: LOG_0046
LOG Titel: Ionic composition of the earth's radiation belts
LOG Typ: article

Übergeordnetes Werk

Werk Id: PPN1015067948
PURL: http://resolver.sub.uni-goettingen.de/purl?PPN1015067948
OPAC: http://opac.sub.uni-goettingen.de/DB=1/PPN?PPN=1015067948

Contact

Niedersächsische Staats- und Universitätsbibliothek Göttingen
Georg-August-Universität Göttingen
Platz der Göttinger Sieben 1
37073 Göttingen
Germany
Email: gdz@sub.uni-goettingen.de

J Geophys (1983) 52:215–238

Journal of Geophysics

Ionic Composition of the Earth's Radiation Belts* **

W.N. Spjeldvik

Cooperative Institute for Research in Environmental Sciences, University of Colorado, Boulder, CO 80309, USA and Nordmann Research Ltd. Boulder, CO 80303, USA

Abstract. Several different ion species have been positively identified in the earth's radiation belts. Besides protons, there are substantial fluxes of helium, carbon and oxygen ions, and there are measurable quantities of even heavier ions. European, American and Soviet space experimenters have reported ion composition measurements over wide ranges of energies: at tens of keV (ring-current energies) and below, and at hundreds of keV and above. There is still a gap in the energy coverage from several tens to several hundreds of keV where little observational data are available. In this review emphasis is placed on the radiation belt ionic structure above 100 keV. Both quiet time conditions and geomagnetic storm periods are considered, and comparison of the available space observations is made with theoretical analysis of geomagnetically trapped ion spatial, energy and charge state distributions.

Key words: Radiation belts – Ion composition – Spacecraft data – Geomagnetic field – Radial diffusion – Charge exchange – Magnetic storms – Ion anisotropy – Trapped radiation.

Introduction

The region of space occupied by the earth's radiation belts contains substantial fluxes of particles ranging in energy from below an electronvolt to above 100 MeV. No single spacecraft particle detector is capable of covering this great energy range, so a combination of detectors must be used, each with its own advantages and limitations. A particularly difficult type of measurement is the mass discriminating detection of ions between a few tens of keV and several hundred keV energies. Instruments that cover these energies have now been devised, but not yet flown in space.

The ionic composition of the radiation belts is both complex and time variable. Besides protons there are substantial fluxes of helium, carbon, nitrogen, oxygen and even heavier ions. Theory predicts that at the higher energies in the MeV range the charge states of these ions should primarily be among the higher attainable. Unlike the energetic electron component of the trapping region, the ion fluxes are generally not distributed into an inner and an outer zone, but rather fill the entire stable trapping region with a peak flux location according to the ion energy. Early in-situ magnetospheric observations unambiguously determined the presence of energetic ions heavier than protons (Krimigis and Van Allen, 1967; Krimigis et al., 1970; Van Allen et al., 1970; Shelley et al., 1972). Subsequent experimental work gave much more detailed information about the distribution of these ions with the observable trapping region parameters: L-shell, energy and pitch angle (Sharp et al., 1974a, b, 1976a, b, 1977a, b, Shelley et al., 1974, 1976a, b, 1977; Johnson et al., 1974, 1975, 1977, 1978; Fritz and Williams, 1973; Fritz, 1976; Fritz and Wilken, 1976; Fritz et al., 1977; Fritz and Spjeldvik, 1978, 1979; Spjeldvik and Fritz, 1978a, b, c, d, 1981a, b, c; Blake, 1973, 1976; Blake et al., 1973, 1980; Blake and Fennell, 1981; Fennell et al., 1974; Lundin et al., 1980; Hovestadt et al., 1972a, b, 1978a, b, 1981; Mogro-Campero, 1972; Panasyuk et al., 1977, Panasyuk, 1980; Panasyuk and Vlasova, 1981). At hundreds of keV and MeV energies, when comparison is made between protons and heavier ions at equal total ion energy, the dominance of the heavy ions is indicated in segments of the radiation belts; on the other hand, flux comparisons at equal energy per nucleon generally favor protons. At lower energies, the recent works of Lundin et al. (1980), Lennartsson et al. (1981), Lennartsson and Sharp (in press 1982) and Young et al. (1982) demonstrate the variability of the ring current ionic composition during different geomagnetic and solar conditions. Significant variations of the high energy trapped ion composition are also known to take place, at least during some magnetic storms (e.g. Spjeldvik and Fritz, 1981a, b, c).

In recent years it has become clear that energetic heavy ions are particularly effective in causing internal damage to spacecraft memory and control systems (J.B. Blake. personal communication, 1980; McNulty, 1981; Adams and Partridge, 1982). Thus the detailed study of these ions is of practical as well as academic interest.

This review is organized into two experimental observation sections where quiet and disturbed time data are presented, a theory section where the physics of ra-

* Based on an invited review paper given at the Symposium on Plasma and Energetic Particles in the Magnetosphere, EGS Meeting, 23–27 August 1982, Leeds, UK

** Work done at the NOAA Space Environment Laboratory, Boulder, Colorado, USA

diation belt heavy ions is outlined together with modeling results, a section comparing these theoretical predictions with the available ion data, and a concluding section that discusses near-future research trends. An unavoidable bias in the selection of papers referred to is due to the author's research inclinations and the fact that it is not possible to read every paper in the field. Observational results from ion mass spectrometers are the subject of the companion review by Young (1983) (see also previous reviews by Shelley, 1979; Johnson, 1979); the present paper will therefore limit its scope to radiation belts ions above ~ 100 keV per ion.

Experimental Observations at Quiet Times

Instrumentation

Significant technological advances in spacecraft borne instrumentation have occurred during the last decade obviating, in many cases, the uncertainty pertaining to the ionic identity. By virtue of the paucity of instruments utilizing solid state detectors, quite complicated detector systems have also been devised. Among the earliest problems were the distinction between energetic ions and electrons, suppression of electromagnetic radiation effects and particles penetrating the sides of the detector head. Ion fluxes can be deduced by comparing the counts in two identical solid state detector systems of which one has a thin metal foil across the entrance aperture, or by having a permanent "broom"-magnet in the collimator of a single detector head or by actively using such a magnet with multiple detectors to form a magnetic spectrometer. To some extent, particle species separation can also be achieved by precise pulse height discrimination. A common type of energetic ion detector flown by numerous groups during the seventies is the twin-element solid state design (Fritz and Cessna, 1975; Panasyuk et al., 1977). By combining the information on the energy deposited in both of the AlSiAu detectors it is possible, within a certain energy range, to determine both ion energy and mass. Such instruments have been flown on numerous spacecraft, and this type of detector system can be operational from several hundred keV per ion to tens of MeV per ion, with ion identification, and down to ~ 14 keV per ion, without mass discrimination, depending on the detector thickness and the design of the adjoining pulse height discrimination system. For measurements of more energetic ions, multiple detector configurations have been designed, generally with increasing detector thickness away from the collimator opening; known absorbers may also be placed between the detector elements (forming a range telescope). Shielding against unwanted radiation can be done by passive means (thick walls) or by an active system (e.g. guard ring scintillators); for a review of energetic particle instruments, see Spjeldvik (1981a).

More modern designs elicit a three parameter ion analysis by measuring both the energy deposited in each of two or more detectors and the time of flight between two of them. From this one obtains a more precise ion identification; however, very fast electronic circuits are necessary in order to measure the particle transit time over path lengths as short as ~ 10 cm or less (Williams et al., 1978). A hybrid instrument combining a proportional counter, solid state detector and a scintillator was successfully used by Hovestadt and Vollmer (1971) on the S3-2 spacecraft for measuring very energetic ions and low energy cosmic rays. A variation of this instrument, which also utilizes an electric field deflection in a 20 kV potential field, was included in the ISEE-1 and ISEE-3 payloads (Hovestadt et al., 1978a). This instrument also permits information about the ionic charge states to be gathered. The energy coverage is primarily in the multi-MeV per ion range. New instruments are currently being developed to extend the data coverage towards lower energies to bridge the gap between the upper energy limit of spacecraft mass spectrometers, which is typically a few tens of keV (Balsiger et al., 1976), and the practical lower energy bound of the mass discriminating solid state detector systems, which is typically 600 keV per ion (Fritz, 1979). Since no data are available from these new instruments, their discussion is deferred to the last section of this review.

The disadvantage with most of the older "proton" (i.e. total ion) detectors is the fact that the ion species remains undetermined. The instruments were most often beam-calibrated with protons, and the mistaken conclusion may be drawn that the observed ions in space are only protons. The latter may only be a valid conclusion in conjuction with other colaborative evidence, such as simultaneous mass-spectrometer or solid state mass discriminating detector data. However, much of the "proton" observation presented in the early literature really represents ion counts within the proton channel passbands, so it is possible that neither the species identification nor the quoted ion energy is correct. This should be kept in mind while re-examining and utilizing older ion ("proton") data.

Radiation Belt Protons

Equatorial observations of radiation belt ion ("proton") fluxes between 78.6 keV and 22 MeV per ion are shown in Fig. 1. These data were obtained with two, separate, twin-element solid state detectors on Explorer 45 (Fritz, 1979; Spjeldvik, 1981a) during the early half of June 1972. The use of a thin solid state detector element for the higher energy passbands and suitable pulse height discriminator logic made most of the data channels insensitive to incident electrons. The ion flux averages shown in this figure (from Fritz and Spjeldvik, 1979) were constructed statistically over ~ 50 quiet-time spacecraft passes, assuming that the ions are indeed protons. Evidence to that effect is only circumstantial; the theoretical calculations of Spjeldvik (1977) demonstrated that the Explorer 45 quiet-time ion data at ~ 100 keV-$\gtrsim 1$ MeV could only be simulated by theoretical calculations if these ions were protons and not helium or oxygen ions. It was also found that the radial flux maximum is systematically displaced towards lower energies with increasing ion energy in this range. Spectrally, the Explorer 45 equatorial ion (proton) observations generally show steep spectra above ~ 100 keV at L-shells beyond $L \sim 4.5$, and a spectral maximum is formed at a few hundred keV at the lower L-shells. Such positive spectral gradients could be un-

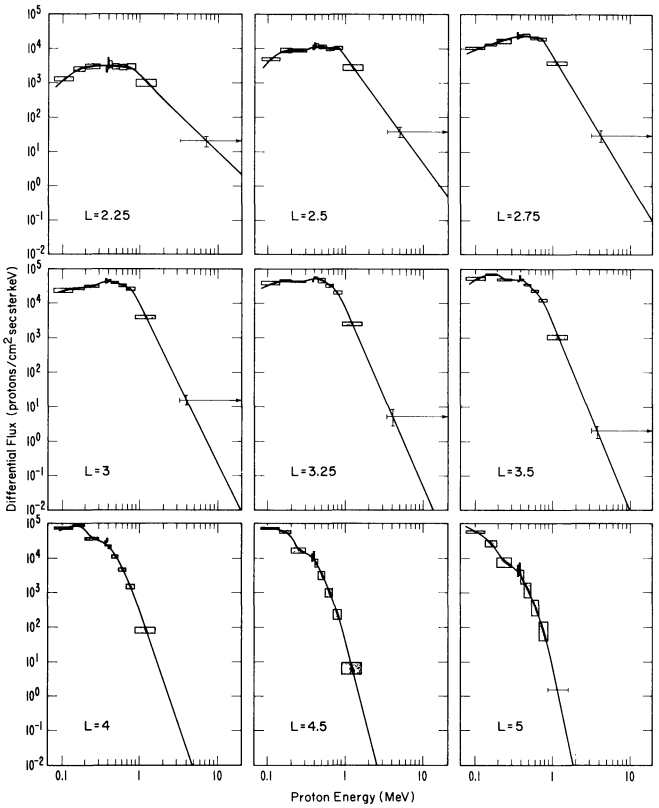

Fig. 1. Energy spectra of equatorial radiation belt protons in the range 0.1–20 MeV deduced from Explorer 45 observations during the geomagnetically quiet period 5–15 June 1972. The data extend over L shell of 2.25, 2.5, 2.75, 3, 3.26, 3.5, 4, 4.5, and 5. The solid curve in each panel is drawn as the best fit to the data points for the differential energy channels and as an analytic approximation to the quasi-integral channel (see Fritz and Spjeldvik, 1979). The data are represented by the energy passband (horizontal extent) and the standard deviations (vertical extent)

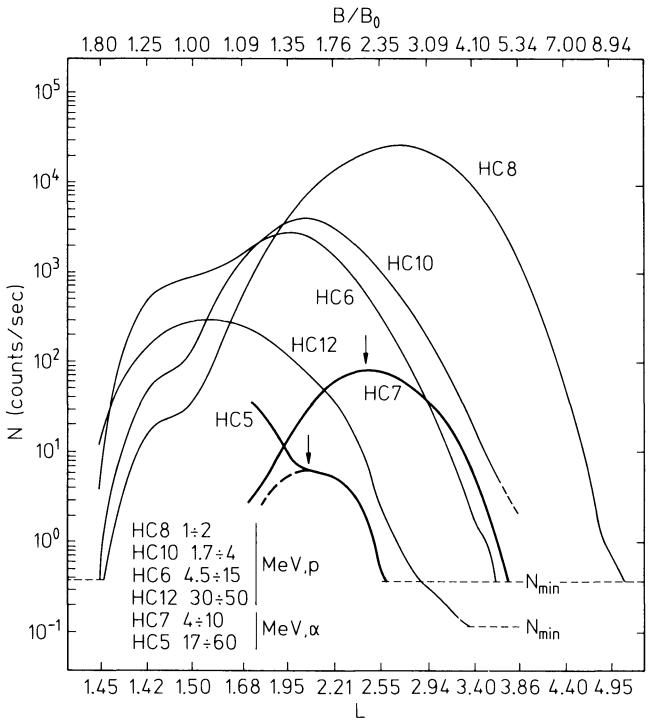

Fig. 2. Ion (proton) observations presented as radial profiles in four passband: HC8 at 1–2 MeV, HClO at 1.7–4 MeV, HC6 at 4.5–15 MeV and HC12 at 30–50 MeV; and alpha-particle (helium ion) observations in two passbands: HC7 at 4–10 MeV per ion and HC5 at 17–60 MeV per ion. The data were obtained with the Molniya-2 spacecraft (for details, see Panasyuk et al., 1977)

stable to plasma wave growth, but that aspect has yet to be fully explored in the radiation blets.

Helium Ions

Instruments capable of discriminating heavy ions form protons have been flown on a number of spacecraft, including Injun-4, Injun-5, Ogo-4, Explorer 45, ATS-6, S3-2, Cosmos-900, Molniya-2 and many others. Figure 2 shows examples of the proton and helium ion results obtained where four of the channels (effective at 1–50 MeV) measured protons and two of the channels (effective at 4–60 MeV per ion) measured helium ions. The orbits of Cosmos-900 and Molniya-2 were such that substantial ranges of B/B_0-values were sampled (B being the magnetic induction at the spacecraft and B_0 its equatorial value on the same field line). When converted to flux units results from this class of instruments have been quite revealing, and we have learned that ions with nuclear charge $Z>1$ can be dominant at certain energies and locations in the trapping region (Fritz and Wilken, 1976; Panasyuk et al., 1977; Fritz and Spjeldvik, 1979). A comparative result from the ATS-6 spacecraft is illustrated in Fig. 3 (from

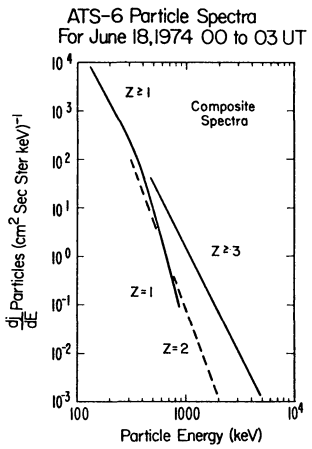

Fig. 3. Equatorial heavy ion spectra monitored with the satellite ATS-6 in the geostationary orbit at $L=6.6$. The instruments did not permit determination of ion charge states but did discriminate between ion mass. The leftward solid curve represents $Z\geqq 1$ ions at $E<350$ keV and $Z=1$ ions (i.e. protons) at higher energies. The simultaneous spectral observations indicate that heavy ions ($Z\geqq 3$) dominates at energies above a few hundred keV per ion. These data are taken during a disturbed period on 18 June, 1974 (from Fritz and Wilken, 1976), but similar results also apply for quiet conditions, (e.g. Spjeldvik and Fritz, 1978b)

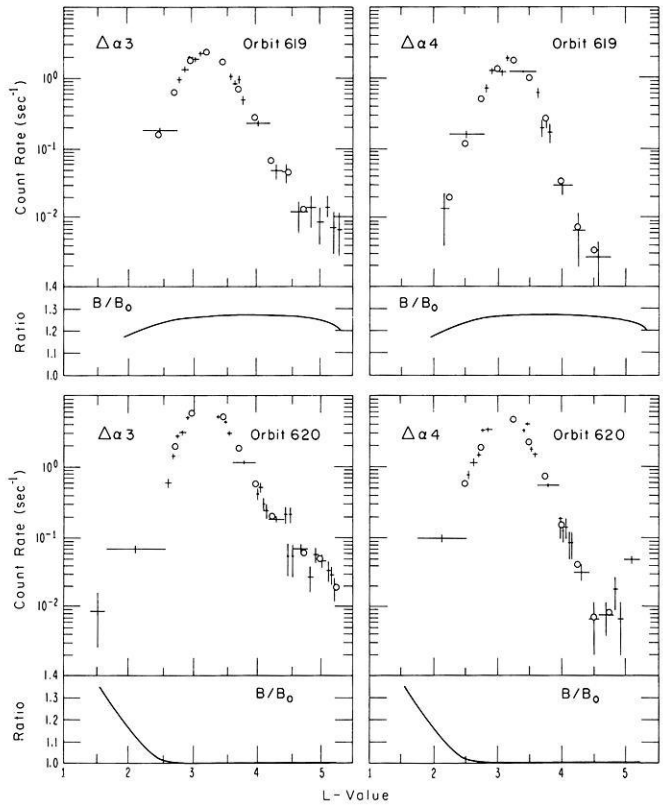

Fig. 4. Radial profiles of helium ions in the earth's radiation belts as observed with Explorer 45 during two consecutive outbound spacecraft passed on June 1, 1972. The passbands are: $\Delta\alpha 3$: 1.16–1.74 MeV per ion and $\Delta\alpha 4$: 1.74–3.15 MeV per ion. The data are represented by crosses where the horizontal error bar indicates the accumulation L-shell interval and the vertical error bars the statistical uncertainty in the data. The circles are interpolation points used in the subsequent analysis. The sub-panels indicate the B/B_0-values of the spacecraft location where $B/B_0=1$ for the exact geomagnetic equator (Fritz and Spjeldvik, 1978)

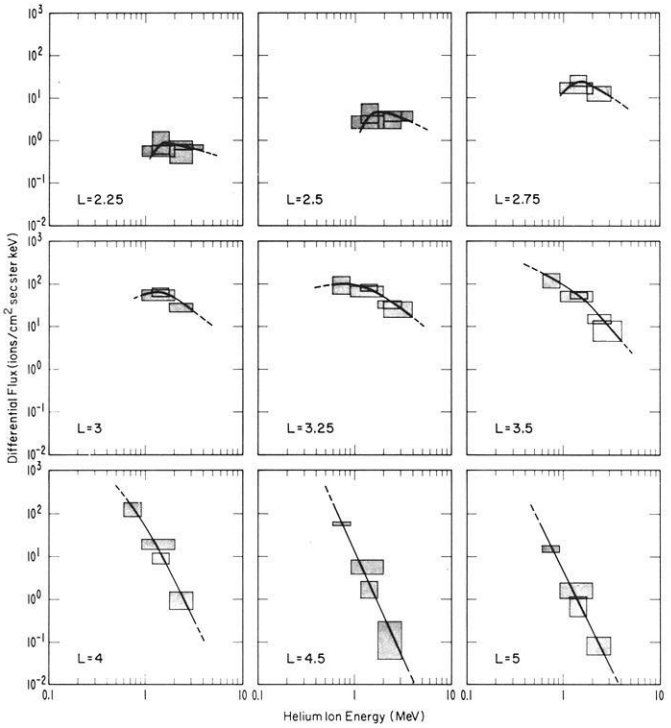

Fig. 5. Energy spectra of equatorial radiation belt helium ions deduced from mass selective ion observations on Explorer 45 during the geomagnetically quiet period 1–15 June, 1972. The spectral coverage corresponds to unambiguous helium ion observations in the $\Delta\alpha 3$ and $\Delta\alpha 4$ channels (1.16–1.74 and 1.74–3.15 MeV per ion) and heavy ion observations ($Z \geqq 2$) in the $\Delta\alpha 1$ and $\Delta\alpha 2$ channels. The data are given at $L=2.25$, 2.5, 2.75, 3, 3.25, 3.5, 4, 4.5 and 5 (Fritz and Spjeldvik, 1979)

Fritz and Wilken, 1976) where measurements of helium ions, CNO (carbon nitrogen, oxygen) ions are compared with those of protons using mass discriminating data channels. It is evident that at this (geostationary) location the $Z>1$ ions dominate over protons when compared at equal total ion energy for energies beyond ~ 1 MeV.

Observations of radiation belt helium ions at the geomagnetic equator over a range of L-shells extending from the top of the atmosphere to $L\sim 5.2$ were made with Explorer 45. Four examples of radial helium ion profiles in the lower MeV energy range are shown in Fig. 4 together with the orbital B/B_0-values (Fritz and Spjeldvik, 1978). Notice that the helium ion count rates are generally higher when the orbit is close to the magnetic equatorial plane (lower panels in this figure). To assess the quiet time structure of radiation belt helium ions, a statistical study was made of ~ 50 Explorer 45 spacecraft orbits through the heart of the trapping region. Fritz and Spjeldvik (1979) found that the radial distributions are fairly narrow with a peak around $L\sim 3.25$ and (full width half maximum) (FWHM) of $\Delta L\sim 0.5$, at energies in the lower MeV range. Ra-

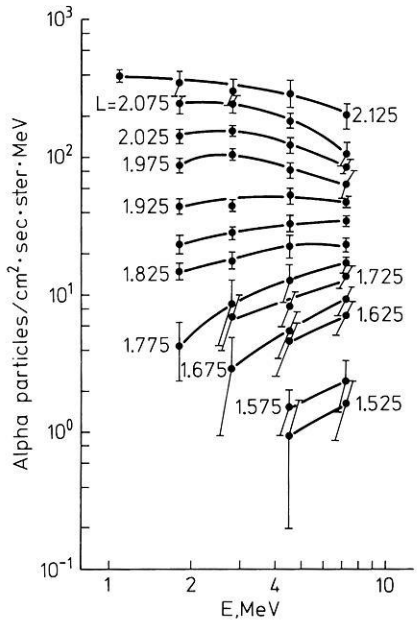

Fig. 6. Differential energy spectra of energetic helium ions in the inner radiation zone. The L-shell coverage extends from $L=1.525$ to $L=2.125$ with $B/B_0\simeq 1.3$. These data were obtained with the OV1-19 spacecraft (from Blake et al., 1973)

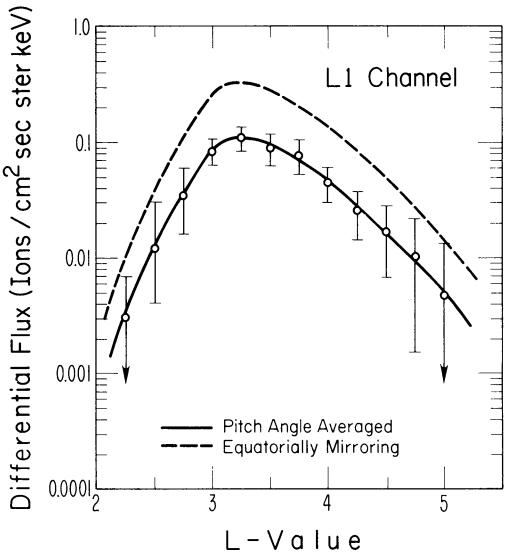

Fig. 7. Radial profile of the Explorer 45 quiet time observations in channel L1 during the period June 1–15, 1972. The *solid line* shows the pitch angle averaged observation, and the vertical error bars indicate the standard deviation in the data set at each quarter integral L shell. The *dashed line* depicts the calculated equatorially mirroring flux assuming that the observed heavy ions are atomic oxygen ions. The energy passband is 1.82–4.8 MeV per ion (from Spjeldvik and Fritz, 1978d)

diation belt helium ion spectra are exhibited in Fig. 5 (from Fritz and Spjeldvik, 1979) where the horizontal error indications depict the width of the passbands and the vertical error bars the statistical uncertainty. Similar to that of protons, the helium ion spectra are found to be quite steep beyond $L \sim 4$, and at lower L-shells a noticeable hardening is seen which results in fairly flat spectra with a possible spectral turnover below $L \sim 3$; the latter cannot be stated with certainty from these data. However, corroborating data at lower L-shells (from Blake et al., 1973) shown in Fig. 6 do indeed demonstrate the positive spectral slopes of MeV helium ions below $L \sim 2$ at the geomagnetic equator.

CNO and Heavier Ions

The pulse height discriminator systems of two element solid state detectors can also be designed to distinguish CNO and heavier ions from the lighter ones, at least at some energies. Fig. 7 depicts the results from Explorer 45 at 1.8–4.8 MeV per ion for CNO ions (Spjeldvik and Fritz, 1978d). It was found that the CNO radial profile is broader than that of helium ions; some of this apparent width could be due to the wide energy acceptance ($\Delta E = 3$ MeV). Unfortunately, only one CNO ion data channel on Explorer 45 had high enough count statistics to be used in the analysis, and this prevents information about the spectral shapes of CNO ions with this spacecraft.

Ions heavier than oxygen could not be determined with certainty from the Explorer 45 instruments during quiet times. Spjeldvik and Fritz (1981c) have placed an upper limit of ~ 0.1 ions/cm^2 s ster integrated over energies beyond ~ 10 MeV per ion for ions with nuclear charge $Z \gtrsim 9$ during the period 1–15 June 1972.

Observations of Carbon and Oxygen Ions in Discrete Channels

The twin detector instruments described in the foregoing are not able to distinguish between the ionic charge

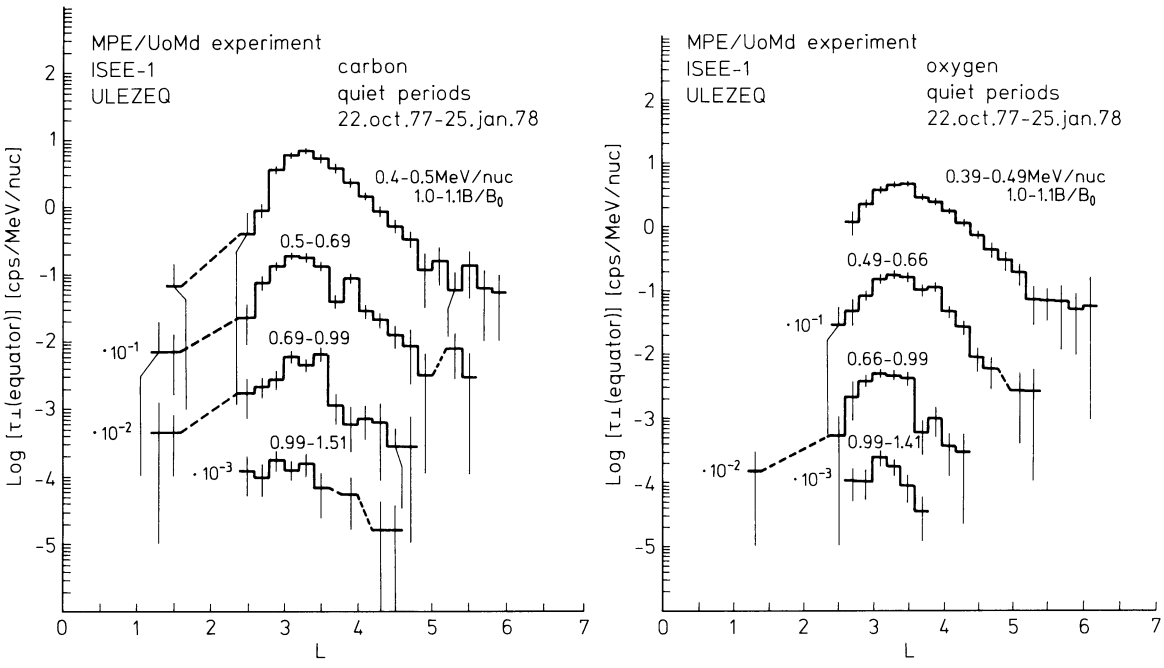

Fig. 8. Observations of carbon and oxygen ions in distinct passbands made with the ULEZEQ detector system on the ISEE-1 spacecraft averaged over a number of selected quiet periods during 22 October 1977 through 25 January 1978.
Left panel: Carbon ion data in four passbands 4.80–6.00, 6.00–8.28, 8.28–11.88 and 11.88–18.12 MeV per ion.
Right panel: Oxygen ion data in four passbands: 6.24–7.84, 7.84–10.56, 10.56–15.84 and 15.84–22.56 MeV per ion (for details, see Hovestandt et al., 1981)

states, and the discrimination between carbon, nitrogen and oxygen ions is also very difficult owing to the similar behavior of these ions in the MeV range. An instrument able to carry out measurements with both mass and charge resolution in the MeV range was flown on ISEE-1. Using data from this instrument, Hovestadt et al. (1978b) were, for the first time, able to report separate measurements of the carbon and oxygen ion fluxes in the earth's radiation belts. This instrument is also capable of measuring helium ions with significant energy resolution at $E=0.39$–2.18 MeV per nucleon in six passbands (multiplication by four gives the total ion energy). As one might expect, they found that the more energetic helium ions have their flux maxima at lower L-shells.

The results for C and O ions deduced from ISEE-1 observations are shown in Fig. 8. For each ion species there are four data channels. For carbon ions these are: $E=0.40$–0.50, $E=0.50$–0.69, $E=0.69$–0.99 and $E=0.99$–1.51 MeV per nucleon, and multiplication by 12 gives the total carbon ion energy passbands. For oxygen ions these are almost identical: $E=0.39$–0.49, $E=0.49$–0.66, $E=0.66$–0.99 and $E=0.99$–1.41 MeV per nucleon, and multiplication by 16 gives the total oxygen ion energy passbands. For both ion species one observes an inward shift of the flux peak location with increasing ion energy. The count-rate comparison also shows that both C and O ions are present in substantial quantities.

Ion Abundance Comparisons

It is of interest to compare the flux intensities of protons with those of the heavier ions, and the relative abundances of the heavy ions. Figure 9 shows the results of calculating the ratio of helium ion flux to that of protons using the Explorer 45 statistical average during 1–15 June 1972 (from Fritz and Spjeldvik, 1979). The shaded areas indicate the estimated uncertainty in the final result. This comparison, which was made at equal total ion energy, demonstrates that the He/p ratio well exceeds unity in the outer radiation zone at the higher energies. At $L=5$, say, the value of this ratio is ~ 10 at 3 MeV per ion. A significant variation of the He/p ratio is also evident in recent Soviet results; Fig. 10 shows data reported by Panasyuk et al. (1977) using observations made with the Molniya-2 spacecraft. Although these data do not pertain to the geomagnetic equator or to fixed B/B_0-values, the same trend is evident, namely a strong increase in the He/p ratio with higher L-shells. The lower part of this figure also shows the observed He/p ratio calculated at equal energy per nucleon for the same spacecraft orbit. Statistical results have also been obtained for the He/p ratio using the Explorer 45 quiet-time observations in the geomegnetic equatorial plane ($B/B_0 \cong 1$). These results, which are shown in Fig. 11, demonstrate that the He/p values at equal energy per nucleon are small, usually in the range $10^{-3\pm1}$ at these L-shells and that a systematic energy variation is seen with a minimum located at several hundred KeV per nucleon. This minimum is not evident in the results of Panasyuk et al. (1977) quoted above, this could be due to the Molniya-2 orbit or it could be a temporal feature dependent on the injection and diffusion pre-history of these particles. One should

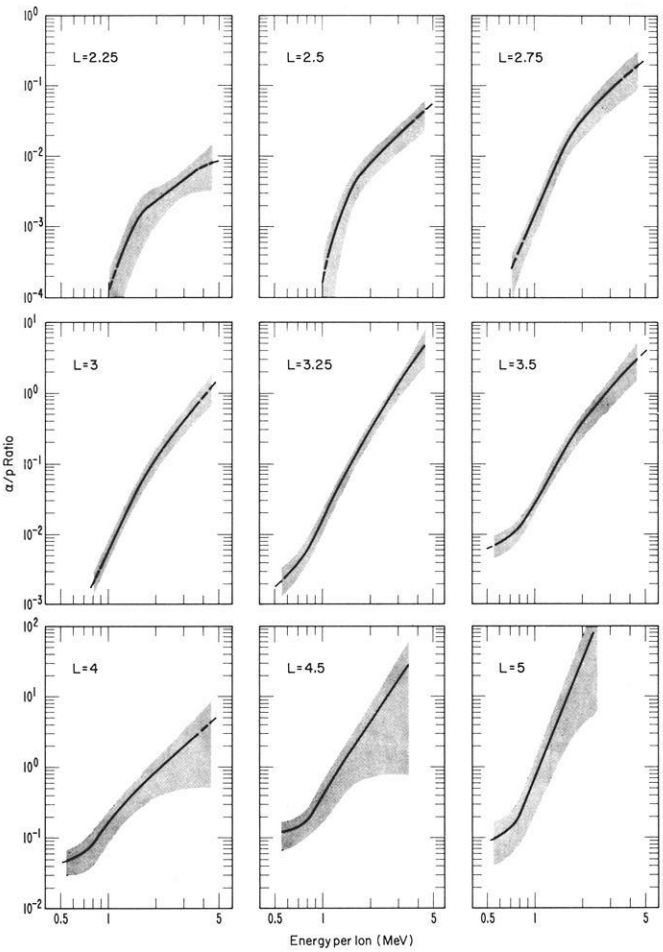

Fig. 9. Calculated quiet time equatorial He/H (or α/ρ) ion flux ratio in the earth's radiation belts during geomagnetically quiet conditions. The data were reduced based on simultaneous ion (most likely proton) and helium ion data obtained with the Explorer 45 spacecraft during 1–15 June 1972. The ratios are given at equal total ion energy in the range 0.5 to 5 MeV per ion, and the shaded areas depict the statistical uncertainty in the derived ratios (Fritz and Spjeldvik, 1979)

point out that the observed He/p ion flux ratio values at equal energy per nucleon are more than an order of magnitude lower than the solar wind He/p abundance ratio which (by number density) can vary from less than 1% to more than 10% with perhaps a mean of $\sim 4\%$ (e.g. Hirschberg, 1973, 1975). For further details of the solar wind ion composition see Bame et al. (1975).

It is of interest to compare the CNO/p ion flux ratio, and the statistical results from Explorer 45 for CNO ions given in Fig. 7 together with the proton data in Fig. 1 yield the comparison (at equal total ion energy) shown in Fig. 12 (from Spjeldvik and Fritz, in press 1982). As in the case of the He/p ratio, the CNO/p ratio at equal energy per ion also shows a significant positive gradient with L-shell, and such that the CNO/p ratio exceeds unity at $L>4.5$. This observed trend, from the 50-orbit statistical data of Explorer 45 during 1–15 June 1972, is also consistent with the ion abundance result from ATS-6 at the geostationary orbit at $L\sim 6.6$ shown in Fig. 8. When compared at equal en-

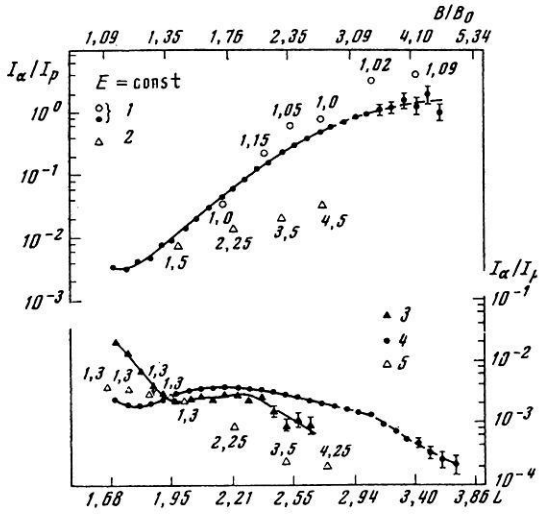

Fig. 10. Determination of the He/H ratio versus L-shell based on data from the Molniya-2 spacecraft and comparison with OV1-19 data. The upper abscissa scale also indicates the B/B_0-values along the Molniya-2 orbit for all solid (filled) data symbols. *Upper curves:* The He/H ratio at equal energy per ion: solid circles are Molniya-2 data at 4.5–15 MeV per ion and open circles are Molniya-2 data for another spacecraft pass closer to the magnetic equator (with B/B_0-values indicated for each data point). Open triangles show the comparative data from OV1-19 at 5.55 to 9 MeV per ion; the B/B_0-values for this spacecraft orbit are also indicated for each data point. *Lower curves:* The He/H ratio at equal energy per nucleon: Solid triangles denote Molniya-2 data at 4.5–15 MeV per nucleon and solid circles denote Molniya-2 data at 1–2 MeV per nucleon. For comparison also OV1-19 data are shown as the open triangles; the B/B_0-values for this spacecraft orbit are also indicated for each data point

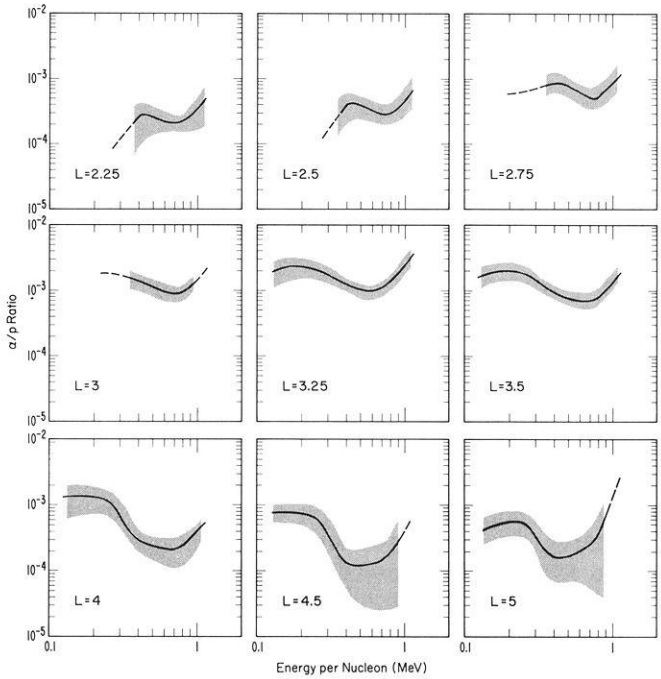

Fig. 11. Calculated equatorial quiet time He/H ion flux ratios at equal energy per nucleon in the earth's radiation belts. The results utilize the same data base as given in Fig. 16, and the shaded areas depict the statistical uncertainty in the derived results

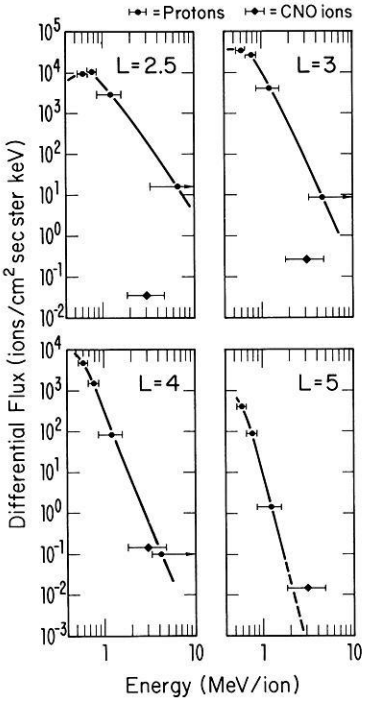

Fig. 12. Comparison of quiet time ion (most likely proton) and CNO ion fluxes in the earth's radiation belts at $L=2.5$, 3, 4 and 5 using simultaneous observations made with Explorer 45 during 5–15 June 1972. The horizontal bars depict the energy passbands for the different ion species (from Spjeldvik and Fritz, 1982)

ergy per nucleon, the CNO/p ratio would be very small throughout most of the radiation belts, however.

It is well known that if the MeV heavy ions in the radiation belts have their origin in the sun (via the solar wind or solar energetic particles) or in low energy galactic cosmic rays then, by the elemental abundance, the geomagnetically trapped C and O ion flux intensities should be roughly comparable. If these ions had their source in the terrestrial atmosphere/ionosphere (via the polar wind and/or upward auroral ion jets followed by acceleration to MeV energies) then the C/O flux ratio would be very small, of the order $\sim 10^{-5}$ (e.g. Blake, 1973). It is here assumed that some unknown (implausible) process does not exist that could strongly favor C over O ions.

It is quite clear that the fluxes of carbon and oxygen ions are of comparable intensity, however; and thus, pending confirmation by independent means, the results of Hovestadt et al. (1978b, 1981) illustrated in Fig. 8 establish the extraterrestrial origin for MeV radiation belt ions. A detailed co-comparison is given in Fig. 13 which gives the C/O flux ratio at equal energy per nucleon. At $L=2.8$–3.8 this ratio varied between 1.3 at 400 keV per nucleon to 4.1 at 1.2 MeV per nucleon. When such comparison is made at equal total ion energy the ratio is about unity (within a factor of two). Although these ISEE-1 results are given for a single pass through the radiation belt trapping region, one would expect to find long term stability during quiet times (as evidenced by the Explorer 45 data discussed above). This contrasts the ion composition results obtained by the mass spectrometers, at tens of keV en-

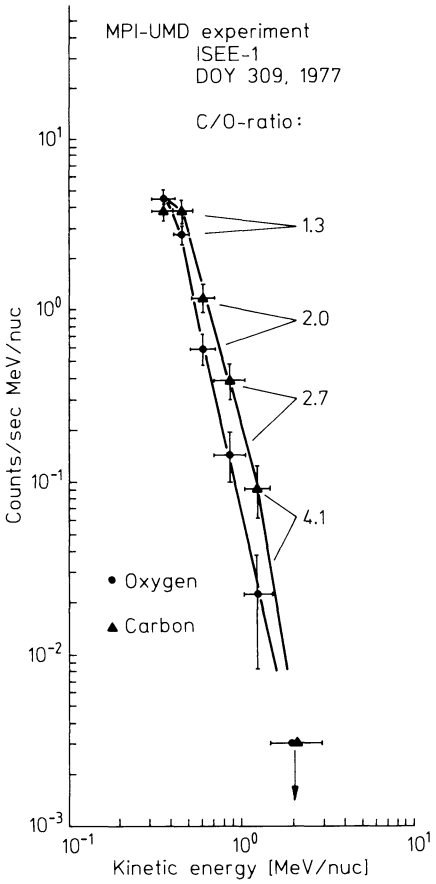

Fig. 13. Direct comparison of simultaneously derived spectra of carbon and oxygen ions in the earth's radiation belts at $L = 2.8$–3.8. The data were obtained with the ULEZEO detector system on the ISEE-1 spacecraft. These comparisons were made at equal energy per nucleon (from Hovestadt et al., 1978b)

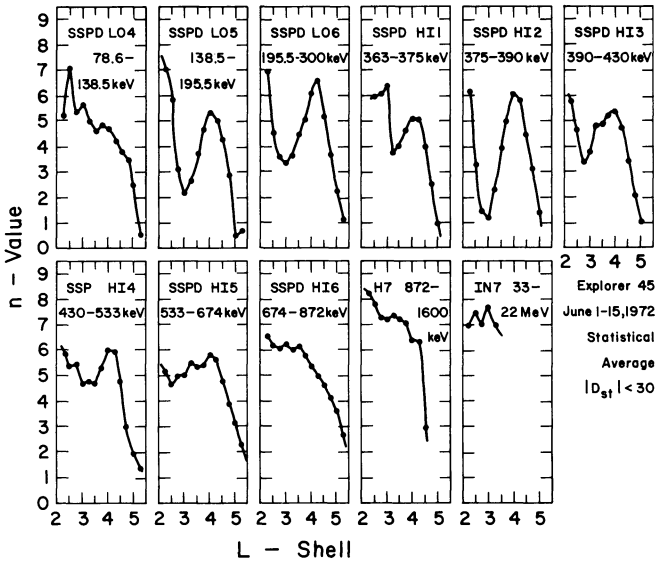

Fig. 14. Determination of the pitch angle anisotropy n-value based on the assumed functional relation $j(\alpha_0) = j(\pi/2)\sin^n \alpha_0$. The data represents a statistical average of ~ 50 Explorer 45 passes through the radiation belts when $|D_{st}| < 30$ nT during 1–15 June 1972

ergies and below. where substantial time variability on the time scale of hours and days in the ionic composition is found (Lyons and Moore, 1981; Lundin et al., 1980; Lennartsson et al., 1981; Lennartsson and Sharp, 1982).

Ion Anisotropies

Observed pitch angle anisotropies of energetic electrons have yielded significant insight into the dynamical processes operating on these particles (Lyons et al., 1971, 1972; Lyons and Thorne, 1973). Studies of anisotropy characteristics of energetic ions could likewise give valuable information about scattering processes and plasma waves such as ion-cyclotron waves. Joselyn and Lyons (1976) have delineated the energy ranges and spatial locations of such interactions for protons; however, much work remains to be done, both from the theoretical and experimental sides, for different ion species.

Specific studies of angular particle distributions have been made by Williams and Lyons (1974a, b), and Lyons and Williams (1975, 1976). Statistically, during a two-week geomagnetically quiet period, the proton anisotropies have been determined from the Explorer 45 data by plotting the observed omnidirectional fluxes versus the B/B_0-parameter (Fritz and Spjeldvik, 1979) and those results show that the proton pitch angle distributions become somewhat more anisotropic with lower L-shells and with higher energies but also that some deviations from a monotonic trend occurs at some L-shells and energies. Plotting these data versus L-shell with $\Delta L = 0.25L$ resolution yields the result shown in Fig. 14. In this graph the B/B_0-dependences have been reduced to a single parameter fit, assuming a functional relation

$$J = J_0 \sin^n \alpha_0 = J_0 (B/B_0)^{-n/2}$$

where α is pitch angle, subscript-0 denotes equatorial ($B/B_0 = 1$) quantities, J is ion flux, and the exponent (anisotropy index) n is the single parameter anisotropy information. One should, of course, be aware that not every pitch angle distribution in the trapping region can be parametrized this way. Injection effects, L-shell splitting, preferential angular scattering at some pitch angles and B-field time variability are examples of processes that may produce other types of angular distributions. Nevertheless, much of the radiation belt ion pitch angle distributions are to a first approximation expressable by such a functional relation. A secondary reason for plotting the proton data this way is that is facilitates direct comparison with other ion species where complete pitch angle distributions may not be available, but where an n-index often can be deduced.

The corresponding Explorer 45 anisotropy record for energetic helium ions in the lower MeV range has been studied by Fritz and Spjeldvik (1978). As in the case of protons, these statistical data appear to be reasonably well matched by the above assumed functional form. For MeV helium ions no systematic L-shell variation of the anisotropy n-index is deduced, and this is

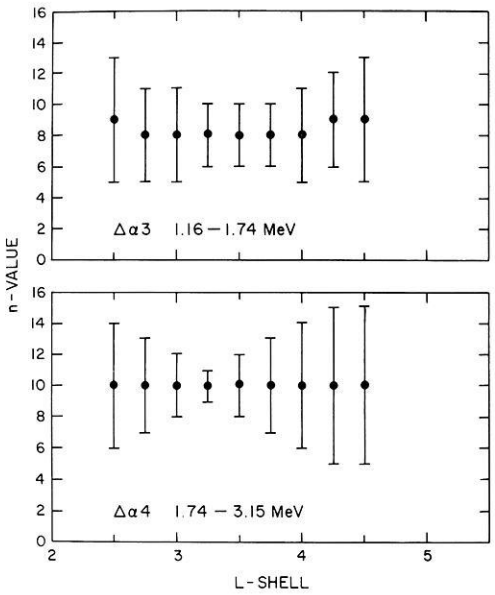

Fig. 15. Equatorial helium ion anisotropy radial profile using the same data as given in Fig. 23 but with a resolution of $\Delta L = 0.25$ from $L = 2.5$ to $L = 4.5$. The n-values are given with estimated errorbars according to the data spread at a given L-shell

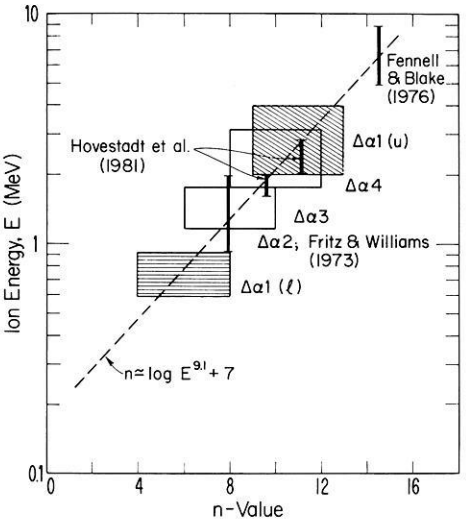

Fig. 16. Equatorial derivation of an empirical energy dependence of the radiation belt helium ion anisotropy index n based on results from several spacecraft. A functional relation $n \simeq 7 + 9.1 \log E$ with E in MeV per ion is deduced (from Fritz and Spjeldvik, 1982)

explicitly illustrated in Fig. 15 (from Fritz and Spjeldvik, 1982) although the errors bars are large enough to allow for significant variation. Of course the energy coverage is limited, and one cannot exclude an $n(L)$-dependence at other helium ion energies. There is, however, a systematic variation of the n-index with helium ion energy. That finding is illustrated in Fig. 16 where a dependence $n(E) \sim 7 + 9.1 \log(E/E_0)$ is deduced with $E_0 = 1$ MeV. This empirical fit appears to provide a fair description of all the Explorer 45, ISEE-1 and S3-2 helium ion anisotropy data within the plasmasphere.

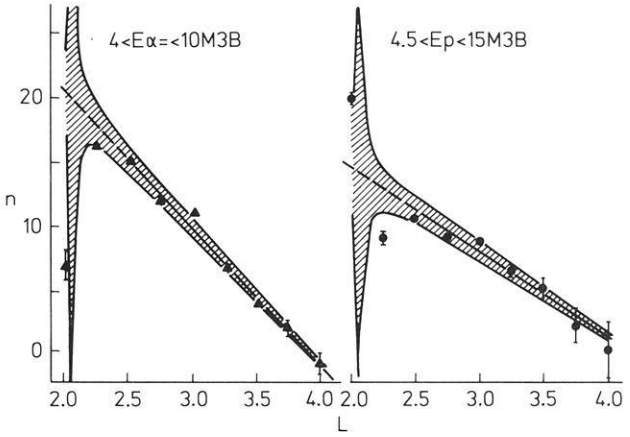

Fig. 17. Pitch angle anisotropy index n versus L-shell of observation, but for varying B/B_0-value with L-shell. The data were obtained with the Molniya-2 spacecraft on 25 October 1975. *Left panel:* n-value versus L-shell for 4–10 MeV per ion helium ions (1–2.5 MeV/nucleon). *Right panel:* n-value versus L-shell for 4.5–15 MeV ions (assumed to be protons) (from Panasyuk and Vlasova, 1981)

In contrast to these results, Panasyuk and Vlasova (1981) have deduced a rather strong dependence of the n-index with L-shell. Their result is reproduced in Fig. 17 and is based on proton and helium ion data from the Molniya-2 spacecraft where wide proton and helium ion data channels, 4.5 –15 and 4–10 MeV per ion, respectively, were used. It is conceivable that at the higher L-shells primarily the lower energy protons and helium ions are measured, while at the lower L-shells the counts would come from the more energetic ions (as one might expect from theoretical considerations). If so, then an energy dependence can be seen as an apparent L-dependence and vice versa. The Molniya-2 data were reduced using only two spacecraft orbits from which a two point anisotropy determination was made; this could leave the result sensitively dependent on the accurate orbit parameters and the magnetic field model; the latter was taken as a dipole. M. Panasyuk (personal communication, 1982) has also pointed out that if the distribution fails to follow a $\sin^n \alpha_0$ dependence at large B/B_0 values then unreliable n versus L determinations could result. The differences between the Explorer 45 and the Molniya-2 results were intriguing enough to pursue the investigation further, however. Figure 18 shows the results of plotting all available helium pitch angle anisotropy information versus L-shell, regardless of the ion energy. The data are clearly significantly less well ordered, and it is difficult to deduce a common L-shell variation of the n-index for helium ions. In particular, the very low n-values deduced by Panasyuk and Vlasova (1981) at $L > 3.5$ (the helium ion fluxes would become isotropic just below $L = 4$) are not supported by the other data. On the other hand, the high n-values observed near $L \sim 2.5$ by these researchers agree well with the observations of Fennell and Blake (1976).

A recent result by Blake and Fennell (1981) indeed shows that a single n-value does not describe the helium anisotropy at large B/B_0-values. Their result is given in Fig. 19 for helium ions at 392–960 keV per ion

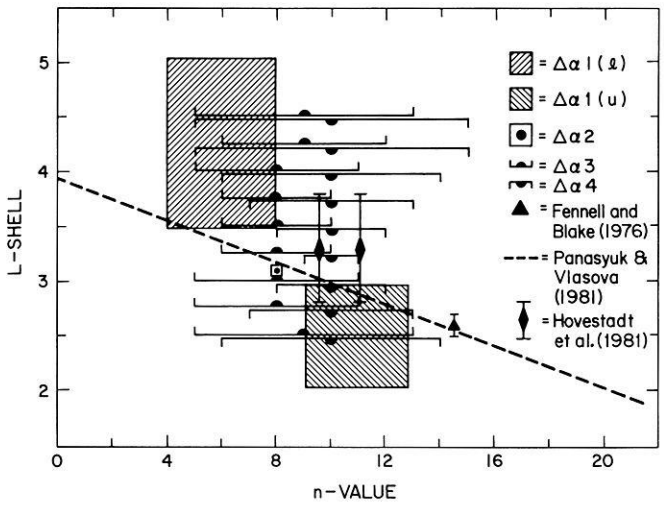

Fig. 18. Plotting of n-value versus L-shell regardless of helium ion energy from many experiments. Explorer 45 quiet time data: $\Delta\alpha 1(l)$ at 0.59–0.91 MeV per ion, $\Delta\alpha 1(u)$ at 2.00–3.99 MeV per ion, $\Delta\alpha 2$ at 0.91–2.00 MeV per ion, $\Delta\alpha 4$ at 1.74–3.15 MeV per ion. Also shown are data from Fennell and Blake (1976), Panasyuk and Vlasova (1981) and Hovestadt et al. (1981)

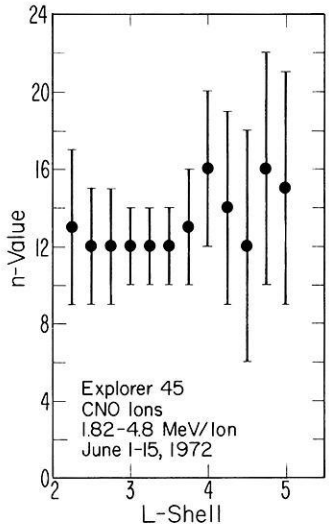

Fig. 20. Variation n-value with L-shell for CNO ions at 1.82–4.8 MeV per ion. The data were obtained with Explorer 45 during the geomagnetically quiet period 1–15 June 1972. To lowest order little significant variation of n with L can be discerned

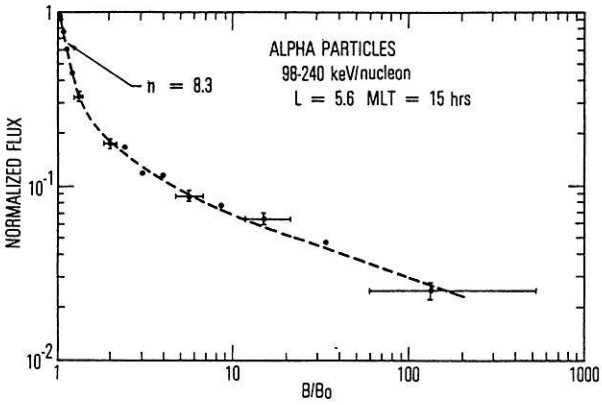

Fig. 19. Anisotropy information at large B/B_0-value for helium ions at 392–960 keV per ion at $L=5.6$ and MLT = 15 hours given by Blake and Fennell (1981). These data were obtained with the SCATHA spacecraft. Notice that a simple relation $J=J_{eq}(B/B_0)^{-n/2}$ is a poor fit to the data at $B/B_0 \gtrsim 2$ while $n=8.3$ is a fair fit at $1 \lesssim B/B_0 \lesssim 2$

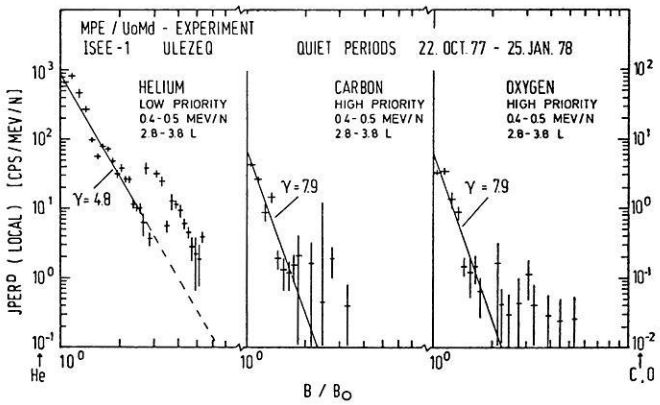

Fig. 21. The observed B/B_0-dependence of helium, carbon and oxygen ions obtained with the ULEZEQ detector system on the ISEE-1 spacecraft. *Left panel:* Helium ion data at 1.6–2.0 MeV per ion (0.4–0.5 MeV per nucleon) for which an n-value of 9.6 ($\gamma=n/2=4.8$) is deduced for $B/B_0 \lesssim 2$. *Middle panel:* Carbon ion data at 4.8–6.0 MeV per ion (0.4–0.5 MeV per nucleon) for which an n-value of 15.8 ($\gamma=n/2=7.9$) is deduced. *Right panel:* Oxygen ion data at 6.4–8.0 MeV per ion (0.4–0.5 MeV per nucleon) for which an n-value of 15.8 ($\gamma=n/2=7.9$) is deduced. The data were averaged over the L-shell interval $L=2.8$–3.8. Notice deviations from the simple $(B/B_0)^{-n/2}$ form at $B/B_0 \gtrsim 2$ (Hovestadt et al., 1981)

(98–240 keV per nucleon) and shows that near the geomagnetic equator the pitch angle anisotropy is describable by $n \sim 8.3$ (for $B/B_0 < 1.6$) while a much smaller n-value describes the larger distances from the geomagnetic equator. Thus, measurements made at varying B/B_0-values would also be expected to give an apparent $n(L)$- dependence, particularly when the B/B_0-range covers the transition between the two different anisotropy levels.

The pitch angle anisotropy is also substantial for CNO ions. In a statistical study of Explorer 45 data, Spjeldvik and Fritz (1978d) found n-values typically in the range 10–12 at 1.8–4.8 MeV per ion (for oxygen ions) on the geomagnetic equator. Figure 20 shows the n-values deduced from these quiet time observations during 1–15 June 1972. To lowest order, there is not a reliable variation of n with L, although some slight non-regularity in the vicinity of $L=4$ to 5 is seen.

Data from the ISEE-1 spacecraft extend the quiet-time ion anisotropy information for a number of different ion species. Figure 21 from Hovestadt et al. (1981) demonstrates that, at comparable energies per nucleon (0.4–0.5 MeV per nucleon), carbon and oxygen ions are substantially more anisotropic than helium ions where $n_{He} \sim 9.6$ and n_C and $n_O \sim 15.8$ measured at L

$=2.8$–3.8. Of course, seen in total ion energy, the carbon and oxygen ions are factors of 3 and 4 times as energetic as the helium ions.

One may conclude that energetic heavy ions in the earth's radiation belts are consistently highly anisotropic.

Observations During Magnetic Storms

A few studies have addressed the radiation belt ion composition during disturbed conditions such as magnetic storms. The qualitative behavior of the proton (ion) component at tens and hundreds of keV energies has long been studied. Davis and Williamson (1963, 1966) found that while lower energy ion fluxes, at tens to hundreds of keV, were enhanced during magnetic storms, higher energy ion fluxes in the MeV range were often decreased. Söraas and Davis (1968) recognized the importance of analyzing the phase space density at fixed first and second adiabatic invariants. Non-monotonic features in radial distributions of the phase space density are attributable to internal sources, "injections" or to time variations in the boundary conditions, i.e. to more rapid flux variations in the outer radiation zone. It is now recognized that the storm-time ion flux enhancements commonly observed at lower radiation belt energies represents the ion injection while the high energy decreases are often due to adiabatic adjustment of the magnetic field. An example of such storm-time variations is shown in Fig. 22 where ion (proton) energy density from Explorer 45 is depicted, and similar variations have been observed with ISEE-1 and other spacecraft (Williams and Lyons, 1974a, b; Lyons and Williams, 1976; Williams, 1980, 1981, in press 1982; Burke, 1981). Open circles depict pre-storm data and closed circles the storm time observations. When these data are reanalyzed in terms of the phase space densities themselves adiabatically mapped by the magnetic field variations (D.J. Williams, personal communication, 1980; Burke, 1981) the high energy flux decreases can be adequately accounted for as being a mere adiabatic adjustment. A similar situation also exists for storm-time energetic electrons (West et al., 1973, 1979, 1981; Spjeldvik and Thorne, 1975; Lyons and Williams, 1975).

Acceleration of pre-existing lower energy particles can in many cases explain "injections" as observed with instruments of finite energy bandwidth. A cross-L non-diffusive displacement preserving the first two adiabatic invariants can appear as a "source" for the geomagnetic storm, main-phase ring current (i.e. Lyons and Williams, 1980). This result emphasizes the need for clear distinction between physical transport from one topologically different region of the magnetosphere to another, on one hand, and essentially in-situ redistribution in velocity space, on the other hand. Both processes have in the past been labeled "injections".

From studies of data obtained by spacecraft in low and high altitude orbits it is recognized that all ion species are not injected proportionally to their pre-storm radiation belt ionic abundance. Randall (1973) has given a detailed account for the observed He/p ratio variations observed at low altitudes during a magnetic storm. Unfortunately, because of the off-equatorial observation location one could not with certainty distinguish between actual abundance variations and species dependent pitch angle distribution adjustments. With data from the later Explorer 45 satellite, in an essentially equatorial orbit, it was recognized that important ionic composition variations do indeed take place during at least some magnetic storms. In a series of papers, Spjeldvik and Fritz (1981, a, b, c) described the variations of the MeV heavy ion fluxes during a sequence of four magnetic storms that occurred during June through December 1972. The D_{st}-record for this time depicts four storm periods with significant D_{st}-excursions by well over 100 nT. The August 1972 magnetic storm differed from the June, September and October/November storms by a quite irregular time hostory of the D_{st}-index. The August 1972 storm was associated with very major solar flares which had significant effects throughout the solar system (Hoffman et al., 1975; Lanzerotti and MacLennan, 1974; Hakura, 1976; Nakagawa, 1976; Bhonsle et al., 1976; Malitson et al., 1976; Rao, 1976; Simnett, 1976; Miller, 1976; Matsushita, 1976; Smith, 1976; Vaisberg and Zastenker, 1976; Intrilligator, 1976; Cahill, 1976; Reagan et al., 1981). Solar wind ions can also be significantly accelerated in shock wave disturbances (e.g. Pesses et al., 1979; Gosling et al., 1980; Scholer et al., 1980).

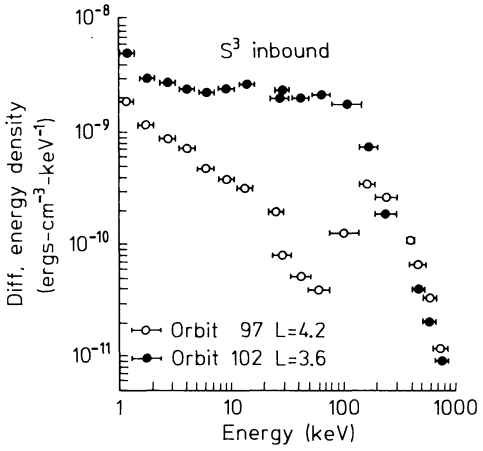

Fig. 22. Stormtime variation of ring current and radiation belt ion energy density observed with Explorer 45 during the quiet time (pre-storm) orbit 97 in December 1971 (open circles) and the stormtime values a day later (orbit 102). Both recordings were made in the interior of the trapping region (from Williams, 1979)

Helium Ion Flux Variations

Enhanced fluxes of energetic helium ions in the MeV range appear fairly suddenly in the heart of the trapping region during at least some magnetic storms. The left panel of Fig. 23 shows the time history of 1.74–3.15 MeV per ion helium ion fluxes at the geomegnetic equator during June through December 1982 at a nominal (undisturbed) $L=3$. These Explorer 45 data show the varying influence of the different magnetic storms on helium ions. Spjeldvik and Fritz (1981a) found that the June 1972 magnetic storm had its principal effect on MeV helium ions beyond $L\sim 3.5$ where the trapped fluxes became enhanced by almost an order of magni-

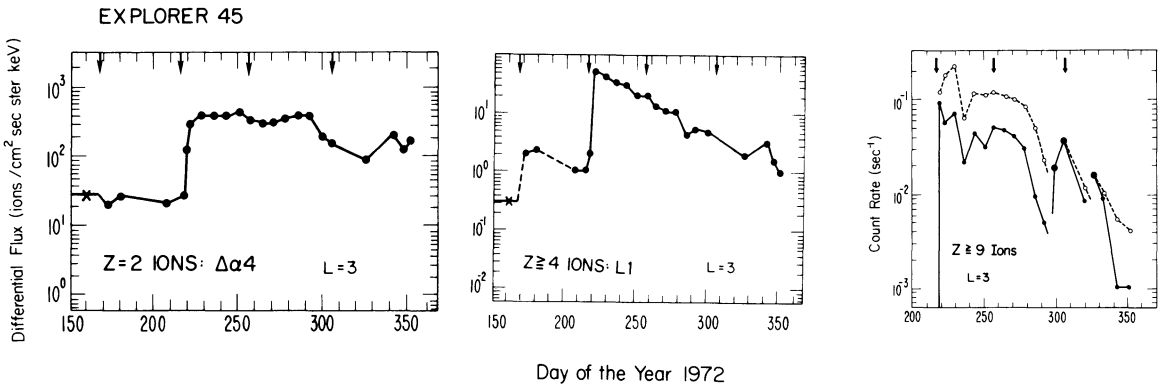

Fig. 23. Evolution of radiation belt helium ion ($Z=2$) and CNO ion ($Z\geqq 4$) flux intensities, and $Z\geqq 9$ ion count rates at 1.74–3.15 MeV per ion, 1.8–4.8 MeV per ion (for oxygen ions) and $\gtrsim 10$ MeV per ion respectively during the four major magnetic storms that occurred during June–December, 1972. The data were obtained with Explorer 45 at $L=3$

tude. At lower L-shells little effect was seen. In contrast, the August 1972 magnetic storm provided a substantial MeV helium ion flux increase onto L-shells well below $L\sim 2.5$. At $L=2.5$ the trapped helium flux enhancement was a factor of ~ 30 while at higher L-shells significant increases were also seen. The subsequent magnetic storms in September and October/-November 1972 produced little observable effects on the MeV radiation belt helium ions below $L\sim 5$. The most likely reason is that any injection provided by these storms was much smaller than that of the August 1972 storm and therefore did not appear evident compared with the prolonged after-effect of the August 1972 magnetic storm. It is possible, of course, that these later two magnetic storms did not inject MeV helium ions. All fluxes are either equatorial ($B/B_0=1$) or have been mapped to $B/B_0=1$ using angular distribution information.

Variations of CNO and Heavier Ions

The corresponding record for MeV CNO ions is shown in the middle panel of Fig. 23. These data pertain to somewhat higher energies, 1.8–4.8 MeV per ion for oxygen ions. The CNO ion flux enhancement was noticeable as low as $L=2.5$ for the June 1972 magnetic storm (Spjeldvik and Fritz, 1981b), and the most prominant increase is seen between $L=3$ and $L=4.5$ for this storm. As in the case of helium ions, the CNO ion fluxes were greatly enhanced during the August 1972 magnetic storm. The relative increase was particularly spectacular at $L\sim 2.5$ where almost three orders of magnitude relative flux enhancement was observed, and a large increase in the trapped fluxes was also seen at $L=3$. In comparison to the August 1972 magnetic storm MeV CNO ion injection, the September and October/-November 1972 magnetic storms provided little changes in the flux levels except possibly at the highest L-shells. The data were mapped to $B/B_0=1$; for details, see Spjeldvik and Fritz (1981b).

While the June 1972 magnetic storm did not provide an enhancement of the fluxes of $Z\gtrsim 9$ ions at $E>10$ MeV above the intensity level observable with the Explorer 45 instruments, the August 1972 magnetic storm provided a substantial injection of the $Z\gtrsim 9$ ions. This is illustrated in the right panel of Fig. 23 which depicts the time evolution of these ion fluxes during and following that storm for a nomial L-shell of $L=3$ at $L<2.5$ and $L>3.5$ the fluxes were generally too low to have usable count statistics. Data on the angular distribution are sketchy, and in this figure an attempt was made to establish the trapped $Z>9$ fluxes at the geomagnetic equator as function of time by mapping the observed fluxes at the actual B/B_0-locations (in the range $1\leqq B/B_0\lesssim 1.4$) to $B/B_0=1$. The dashed line shows the result of that exercise assuming a relation $J=J_0\sin^{10}\alpha_0$ (for details, see Spjeldvik and Fritz, 1981c). Although there are sufficient count statistics to establish the presence of these ions, some of the non-smoothness also results from the small number of counts, at best a few counts per minute. The precise identity of these ions could not be determined with the Explorer 45 heavy ion detector telescope, but expectations from the solar energetic particle emission observations at higher energies (i.e. Webber et al., 1975) suggest that magnesium and silicon ions might be the ones observed. The instrument was not able to distinguish between heavy (atomic) ions such as ions of Mg, Si, Fe etc., and molecular ions (from the lower ionosphere) such as NO^+, O_2^+, etc.; no known mechanism is capable of accelerating ionospheric ions to tens of MeV energies in the earth's radiation belts, however. It is nevertheless worth noting that very energetic molecular ions have been observed in Jupiter's magnetosphere (i.e. Hamilton et al., 1980). A detailed study of solar particle anisotropy, rigidity spectra and propagation characterisitcs for a different event has been carried out by Debrunner and Lockwood (1980), and MaSung et al. (1980) report mean ionization states of energetic particles in the vicinity of the earth's magnetosphere. The charge states of these ions are found to be high, and comparable to those of the solar corona (c.f. Jordan, 1969).

Observed Post-Storm Ion Flux Decay

From the time evolution of the heavy ion fluxes, a typical post-storm ion flux decay time may be estimated. When the time evolution is transport dominated it is of interest to determine whether the net radial diffusion is

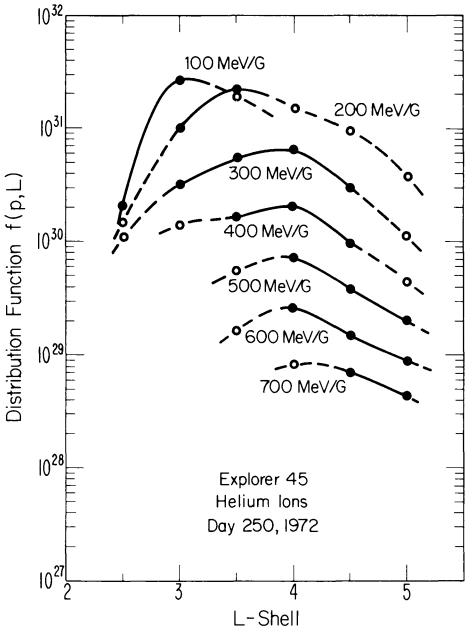

Fig. 24. Distribution function $f(p,L)$ for day 250 (Sept. 6), 1972, calculated from the MeV helium ion flux observations made by Explorer 45 in the Earth's radiation belts. Solid lines and solid circles are from interpolations in the observed data, dashed lines and open circles are from graphic extrapolations in the spectral plots. With the flux $j(E,L)$ given in ions/cm^2 s sr keV the distribution function $f(p,L)=p^{-2}j_1(E.L)$ is plotted in units of ions s/cm^4 g^2 sr keV; multiplication with 6.25×10^8 gives cgs units (ions s^3/g^3 cm^6)

inward or outward. The equatorial net radial diffusion flux can be determined from $\Phi=-D_{LL}L^{-2}\dfrac{\partial f(\mu,L)}{\partial L}$ where $f(\mu,L)$ is the instantaneous ion distribution function at equatorial pitch angle $\alpha_0=\pi/2$. When $\partial f/\partial L>0$ net inward transport is indicated, and that is usually the case during quiet times when the radiation belt internal losses are offset by inward diffusion across an outer zone boundary location. When $\partial f/\partial L<0$ net outward radial diffusive transport is indicated. Figure 24 shows the deduced helium ion radial profile of the distribution function for a range of μ-values corresponding to energies in the lower MeV range. It is clear that beyond $L\sim3$ the $\partial f/\partial L$ values are generally negative showing net outward helium ion transport during the post-storm period following the August 1972 magnetic storm period. Since generally the radial diffusion coefficient increases strongly with higher L-shells ($D_{LL}\sim L^{10}$ for magnetic radial diffusion, e.g. Schulz and Lanzerotti, 1974), cross-L transport can be an important loss mechanism for MeV ions during this period. Eventually the MeV ions diffusing out from beyond $L\sim3.5$ will encounter the magnetopause (on the dayside) or the magnetotail (on the nightside) and thus be lost from the trapping region.

Figure 25 depicts the observed helium ion, CNO ion and $Z\geqq9$ ion decay times. The helium ion decay times, shown in the left panel, vary from ~7 days at $L=5$ to >100 days at $L\sim2.5$. A comparison with theoretical predictions based on Coulomb collision energy degradation, ion charge exchange loss times and typical cross-L transport time scale is also provided. In this context it should be noted that the Coulomb energy degradation times used here are just those of single particle energy degradation, i.e. $\tau_{cc}\sim\left(\dfrac{1}{E}\dfrac{dE}{dt}\right)^{-1}$. In principle, the actual time scale would be the ensemble average determined from the distribution function itself, i.e. $\tau_{EA}=f\left(\left\langle\dfrac{\Delta E}{\Delta t}\right\rangle\dfrac{\partial f}{\partial\mu}\dfrac{\partial\mu}{\partial E}\right)^{-1}$, and such a refinement should be included in future work. The charge exchange loss times were calculated from an assumed (theoretical) distribution over the ionic charge states. While helium ions are subject to at least three different charge state altering reactions, $He^+\rightarrow He^{++}$, $He^{++}\rightarrow He^+$ and $He^+\rightarrow He$, only the last of these produces loss of the ion by "untrapping" it from the magnetic field control. Thus the charge exchange loss rate is determined, in part, from the relative distribution in the different ionic charge states $\tau_{CE}=\tau_{10}(f_1/\sum_i f_i)^{-1}$ where the distribution function subscripts denote the charge state numbers. τ_{10} is just $(\sigma_{10}V[H])^{-1}$ where σ_{10} is the charge exchange cross section for $He^+\rightarrow He$, V is ion speed and $[H]$ is the neutral hydrogen exosphere number density. For the Explorer 45 helium ion channel used in Fig. 25 (1.16–1.74 MeV per ion) a good agreement between the observed post-storm decay times and theoretical expectations is found; similar agreements were found for other helium ion energies (Spjeldvik and Fritz, 1981a).

This type of analysis was also done for CNO ions, and the results were compared with theoretical time scales for oxygen ions. The observed decay times varied from ~6 days at $L=5$ to ~40 days at $L=3.5$. This is shown in the middle panel of Fig. 25 for the 1.8–4.8 MeV per ion CNO data. At first glance it might seem that the observed decay times are longer than the theoretically predicted Coulomb collision times at $L<4$. However, the CNO data channel is quite wide, and it is expected that the CNO ion fluxes within this energy range should be primarily >4 MeV ions at $L<3$ while primarily <2 MeV ions at $L>4$ (Spjeldvik and Fritz, 1978d, 1981b). Thus, invoking this theoretical spectral expectation, the decay data are indeed consistent with theory.

It is more difficult to analyze the $Z\gtrsim9$ ions since the ion identity is unknown and there is also a lack of information about the basic charge exchange cross sections of such ions ($Z\gtrsim9$) in an atomic hydrogen gas. For a review of known cross sections, see Claflin (1970) and Spjeldvik (1979), and references therein. The actual observed decay time scales for the >10 MeV, $Z\gtrsim9$ ions are shown in the right panel of Fig. 25 with error bars corresponding to the uncertainty in the data given in Fig. 23. The decay times range from ~13 days at $L=3.25$ to ~54 days at $L=2.25$. Typically these decay times are short, on the order of a few tens of days with a monotonic decrease of the time scales with higher L-shells. A comparison with the expected cross-L transport times in Fig. 25 reveals that at the L-shells where the $Z\gtrsim9$ ion data were obtained $\tau_{decay}\ll\tau_{diffusion}$. On the other hand, both $\tau_{Coulomb}$ and $\tau_{charge\,exchange}$ should increase with increasing L-shell (because of the decreasing

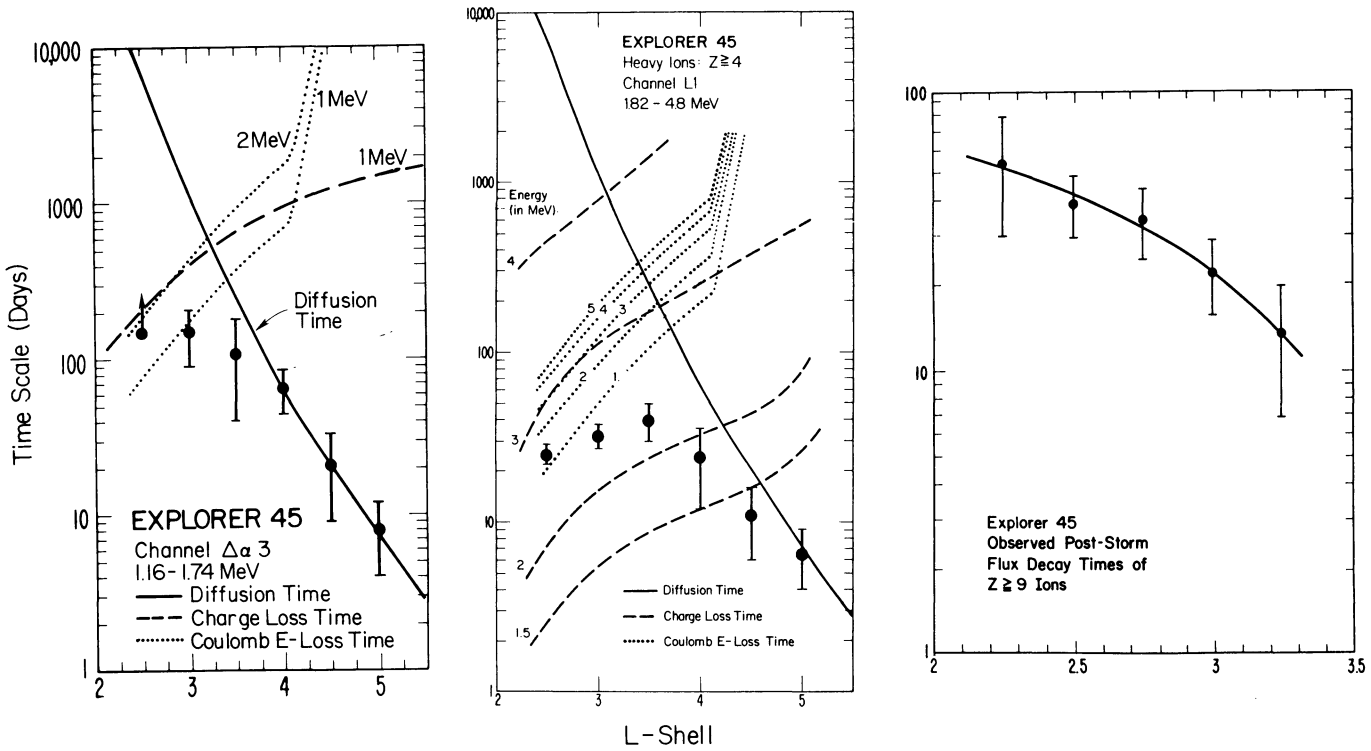

Fig. 25. Time scales of the observed helium ion, CNO ion and $Z \geqq 9$ ion decay following the August 1972 magnetic storm ion injection. The three panels show the data for the $\Delta\alpha 3$, $L1$ and $Z \geqq 9$ ion channels at 1.16–1.74 MeV per ion for helium, 1.8–4.8 MeV per ion for oxygen and $\gtrsim 10$ MeV per ion for $Z \geqq 9$ ions respectively. The vertical error bars show the estimated uncertainty in the time scale determination stemming from statistical variations and the infrequent 'accelerated' mode data sampling. Time scales longer than ~ 3 months cannot unambiguously be determined because of the statistical spread. Likewise time scales shorter than a few days are difficult to resolve. The solid lines are lines of deduced radial diffusion times following an L^{-10} dependence and normalized to the data; and from the helium ion decay record one may estimate radial diffusion times of $6.67 \times 10^7 L^{-10}$ days on L shells well beyond $L = 3.5$ with corresponding uncertainty as indicated by the error bars. Theoretical charge exchange and Coulomb energy degradation times scales are also shown (dashed and dotted lines); for details, see Spjeldvik and Fritz (1981a, b, c)

exospheric neutral atomic hydrogen concentration [H]). Thus it would appear that the theory used so far successfully for He and CNO ions at a few MeV energies cannot explain the decay of the $Z \gtrsim 9$ ions at $E \gtrsim 10$ MeV per ion. The reason for this was suggested by Hoverstadt et al. (1981) who pointed out that the gyroradii for these very energetic heavy ions become so large that the Alfven criterion for the validity of the adiabatic radiation belt approximation is no longer fulfilled. These ions are thus exhibiting a non-adiabatic (or quasi-adiabatic) behavior for which the theory still has to be developed, for example by studying the non-adiabatic ion trajectories (e.g. Störmer, 1955). The net result might be to lower the residence times in the trapping region.

Theoretical Considerations

Theoretical studies of the motion of high energy particles in the earth's magnetic field were carried out early in the century by Störmer and his contemporaries; their work, summarized in the book by Störmer (1955), followed the single particle trajectory tracing approach. The particles were thought to originate in the sun and follow deterministic trajectories in the earth's dipolar-like magnetic field. In the general case, this is a difficult mathematical problem, and even for a static geomagnetic field, no explicit analytic solution has been found. Great simplification can be achieved over much of the energy range of interest for the earth's radiation belts when the three approximate periodic motions of trapped particles are considered (Alfven and Fälthammar, 1963). The fluctuating nature of the geomagnetic field causes perturbations in these periodic motions, leading to particle energy changes, pitch angle scattering and radial transport. The general theory for these processes is well established, e.g. reviews by Fälthammar (1968), Hess (1968), Roederer (1970), Schulz and Lanzerotti (1974), Schulz (1975), Spjeldvik (1979), Lyons (1979). Calculations of radiation belt particle fluxes have also been carried out based on the diffusion theory (Nakada and Mead, 1965; Cornwall, 1972; Lyons and Thorne, 1973; Spjeldvik, 1977; Spjeldvik and Fritz, 1978a, b; Spjeldvik, 1981b).

The recognition that heavy ions play an important role in the radiation belts has led to greater emphasis on the precise ionic composition (Cornwall and Schulz, 1979) and to consideration of the different ionic charge states (Spjeldvik, 1979). In the following the current status of radiation belt ion modeling is outlined, emphasizing the macroscopic properties and the use in developing predictive models of the inner magnetosphere.

Trapped radiation belt ions are subject to fluc-

tuations in the large scale geoelectric and geomagnetic fields, and they may interact with various modes of plasma waves. In a macroscopic sense, this leads to radial diffusion and pitch angle diffusion. Energy degradation by Coulomb collisions cause a "flow" in velocity space and charge exchange reactions may lead to sudden untrapping of the ions. The overall effect of these processes may be written as a multi-mode diffusion equation

$$\frac{\partial f_i}{\partial t}=\frac{\partial}{\partial\phi}\left[D_{\phi\phi_i}\frac{\partial f_i}{\partial\phi}\right]+\frac{\partial}{\partial z}\left[D_{zz_i}\frac{\partial f_i}{\partial z}\right]+\frac{\partial}{\partial J}\left[\left\langle\frac{\Delta J}{\Delta t}\right\rangle_i f_i\right]+\frac{\partial}{\partial\mu}\left[\left\langle\frac{\Delta\mu}{\Delta t}\right\rangle_i f_i\right]+\sum_j \Lambda_{ji}f_j-\sum_j \Lambda_{ij}f_i+S_i. \quad (1)$$

S represents a particle source internal to the trapping region, and μ, J and ϕ are the three adiabatic invariants, z is the canonical pitch angle variable where $z=\phi y'T(y')\,dy'$ and $y=\sin\alpha_0$ where α_0 is the equatorial pitch angle and z is given approximately by

$$z\approx 1/2(1-y^2)\,T(0)-\tfrac{4}{11}[T(0)-T(1)](1-y^{11/4})$$

with $T(y)$ being the bounce time dependence of equatorial pitch angle (Hamlin et al., 1961; Schulz, in press 1981). $\langle\Delta J/\Delta t\rangle_i$ and $\langle\Delta\mu/\Delta t\rangle_i$ are the stochastic degradation rates in the μ and J invariants caused by Coulomb collisions and Λ_{ij} is the charge exchange factor for transformation from state i to state j (e.g. Cornwall, 1972; Spjeldvik, 1979). For protons there is just one charge state ($i=1$) and the last two terms reduce to $-\Lambda_{10}f_1$. Although it is, in principle, possible to solve this equation, there is no analytic solution expressable by a known function for the general case. Even a purely numerical solution is laborious since a four-dimensional parameter space spanned by μ, J, ϕ and i plus time must be considered. The solution in this general case has not yet been obtained, and every numerical simulation has studied simplified cases. A steady-state time independent approximation is most often used.

Lyons and Thorne (1973), in their steady state radial diffusion study of radiation belt electrons, replaced the pitch angle diffusion term with $\frac{\partial}{\partial z}\left[D_{zz_1}\frac{\partial f_1}{\partial z}\right]\simeq -\frac{f_1}{\tau_p(E,L)}$ where $\tau_p(E,L)$ is the overall electron precipitation lifetime versus scattering into the atmospheric bounce loss cone. They also replaced $\frac{\partial}{\partial\mu}\left(\left\langle\frac{\Delta\mu}{\Delta t}\right\rangle f_1\right)$ by $-\frac{f_1}{\tau_{coul}}$ where τ_{coul} is the single particle Coulomb collision "life time" defined from $\tau_{coul}\simeq\left(\frac{1}{E}\frac{dE}{dt}\right)^{-1}$. Of course, the correct ensemble time scale for an arbitrary equatorial pitch angle α_0 is defined as

$$\tau_{EL}=\left(\frac{1}{f_i}\left[\frac{\partial}{\partial\mu}\left(\left\langle\frac{\Delta\mu}{\Delta t}\right\rangle_1 f_1\right)+\frac{\partial}{\partial J}\left(\left\langle\frac{\Delta J}{\Delta t}\right\rangle_1 f_1\right)\right]\right)^{-1},$$

but such a quantity cannot be specified a priori since it depends on the solution to the diffusion problem itself. For electrons there is no charge exchange process to consider. A significant simplification also comes from considering only one pitch angle, most often the equatorially mirroring particles only (i.e. where $J\equiv 0$) are studied. These considerations reduced the electron problem of Lyons and Thorne (1973) to a one-dimensional approximate case of radial transport only. Although the accuracy of some of their simplifications may be called into question, their solution retained much of the essential physics, and they obtained results in good agreement with in-situ electron observations.

In modeling protons and other ions Nakada and Mead (1965), Cornwall (1972), Blake et al. (1973), Spjeldvik (1977) and Spjeldvik and Fritz (1978a, b) retained the radial diffusion term, the Coulomb collision term, and the charge exhange term(s). But they also restricted attention to equatorially mirroring ions, and for energetic ions the pitch angle scattering term was neglected altogether (by assuming $D_{zz}\sim 0$). Figure 26 shows an ex-

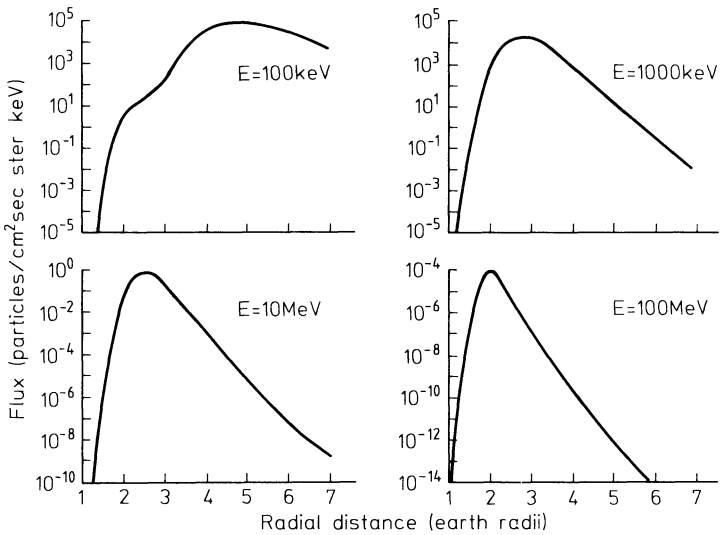

Fig. 26. Theoretical radial profiles of energetic radiation belt proton fluxes calculated from the steady state model of Spjeldvik (1977) with outer radiation zone boundary conditions assigned at $L=7$. The results are shown for 100 and 1,000 keV, and 10 and 100 MeV. These curves were computed based on the exospheric neutral hydrogen model of Tinsley (1976) and with radial diffusion coefficients as described in Spjeldvik (1977). No pitch angle scattering was allowed and only equationally mirroring protons were considered

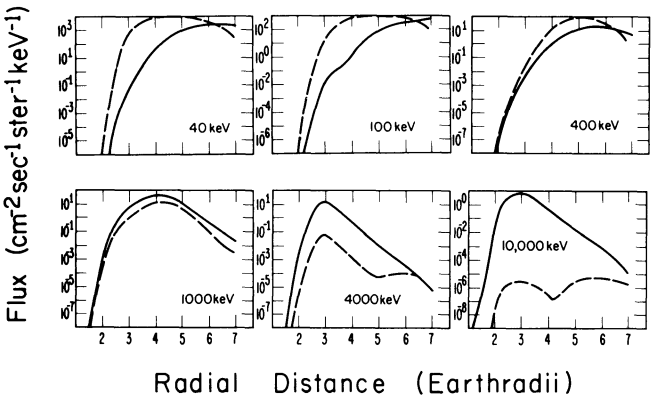

Fig. 27. Theoretical radial profiles of radiation belt helium ion fluxes calculated from the steady state model of Spjeldvik and Fritz (1978a) with outer zone boundary conditions assigned at $L=7$. Dashed curves depict charge state 1 (i.e. He^{+}) while solid curved depict charge state 2 (i.e. He^{++}), and the curved are given for 40, 100, 400, 1,000, 4,000 and 10,000 keV per ion. The relative charge state distribution indicates the dominance of He^{++} above ~ 1 MeV per ion while He^{+} are most abundant at lower energies

ample of the proton model result for $\alpha_0=\pi/2$ (from Spjeldvik, 1977). These calculations reproduce the well known observational result that protons are not distributed into two belts, but occupy a single radiation zone encompassing the entire trapping region, and such that the more energetic protons have their flux peak at the lower L-shells. Spectrally, these calculations show that the proton spectra in the interior of the radiation belts turn over and exhibit positive $\partial j/\partial L$-values (with $j(E,L)=p^2f(p,L)$ where p is the proton momentum) at the lower energies.

A similar treatment of energetic helium ions gave the theoretical distributions illustrated in Fig. 27 (from Spjeldvik and Fritz, 1978a): Notice that the lowest helium ion charge state is dominant below ~ 1 MeV while the second charge state is most important above this energy. This result is essentially independent of the ion charge state boundary condition applied in the outer radiation zone, thus charge state redistribution processes resulting from collisions between the energetic ions and exospheric particles are important in most of the trapping region. Qualitatively the theoretical helium ion fluxes also peak at lower L-shells with increasing ion energy, and their spectra show positive $\partial j/\partial L$-values below ~ 1 MeV at $L \lesssim 3.5$. Some interesting spectral features arise from the combined influences of energy-dependent radial diffusion and energy dependent losses. The parameter used for radial diffusion (Cornwall, 1972) leads to preferential loss of helium ions at ~ 100–1,000 keV total ion energy; for details, see Spjeldvik and Fritz (1978a). The theoretical results are probably not strictly valid below ~ 100 keV since convective processes may be more important than diffusion at and below ring current energies.

Two examples of model results for oxygen ions are depicted in Fig. 28. In the left panels a flux boundary condition was imposed at $L=6.6$ under the assumption that only O^{+} was present (corresponding to a purely ionospheric ion source at all energies), and in the right

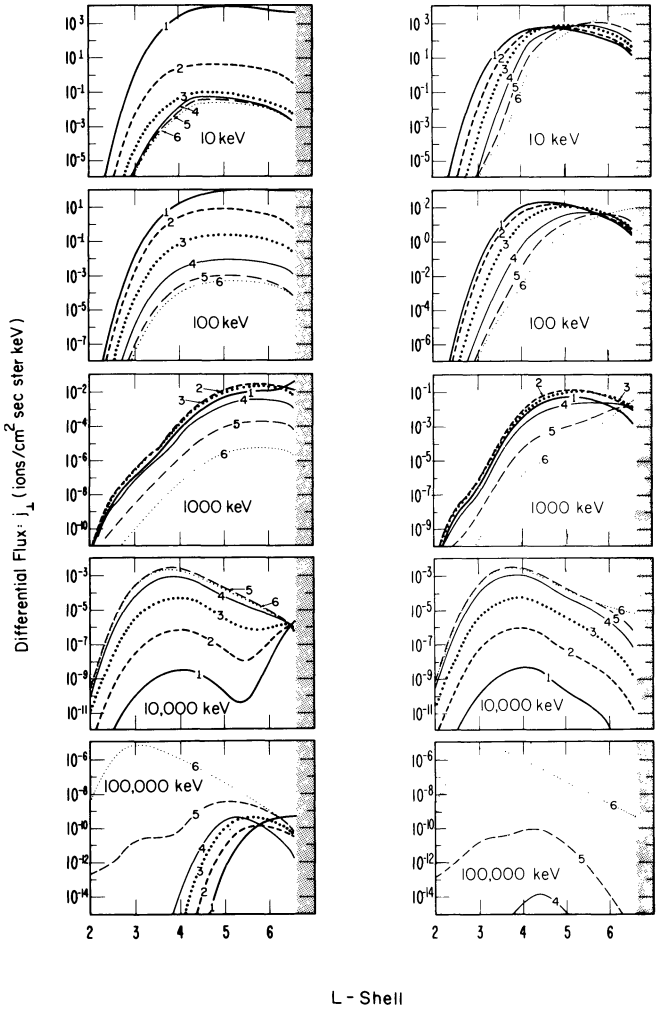

Fig. 28. Computed atomic oxygen ion fluxes in the earth's radiation belts assuming an ionospheric source of O^{+} at the outer zone boundary *(left panels)* or alternating a solar source of O^{6+} ions at the outer boundary *(right panels)*. The six lowest positive charge states are permitted, and the diffusion coefficients have the same values as in the calculations in Figs. 26 and 27. Charge state numbers are given on the curves. The panels show radial profiles at 10, 100, 1,000, 10,000 keV per ion. Detailed description of the theoretical calculations are found in Spjeldvik and Fritz (1978b)

panels the identical spectra were taken at $L=6.6$ but with solely O^{6+} present (an implicit assumption of an extraterrestrial ion source). The calculated oxygen ion fluxes and charge state distributions in the interior of the radiation belts were found to be fairly similar in both cases, however, except near the outer zone boundary. This is explicitly shown in Fig. 29 for 4 MeV oxygen ions subject to the ionospheric (left panel) and solar wind (right panel) source assumptions. Notice that below a charge state redistribution zone of width $\Delta L \sim 1.5$ L-shell units a characterisitc charge state distribution is formed. In this case with O^{4+} ions dominant. For specific details about expected charge state distribution properties and the uncertainties in the calculations from which they are derived, see the review by Spjeldvik (1979).

In all the model calculations carried out so far for

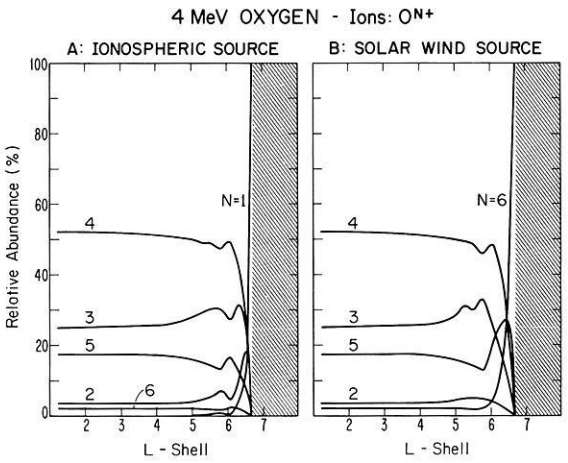

Fig. 29. Normalized charge state distributions for 4 MeV atomic oxygen ions in the Earth's radiation belts. The left panel assumes solely O^+ in the outer radiation zone and the right panel assumes solely O^{+6} at $L=6.6$, corresponding to ionospheric and solar wind ion sources respectively. It can be seen that at L-shells below a narrow transition zone ($\Delta L \sim 1.5$) the charge state distributions become practically independent of the ion source characteristics and that at this energy the fourth charge state predominates the charge state distribution

radiation belt ions, rates of radial transport due to fluctuations in the large scale electric and magnetic fields have assumed that the fluctuation power spectra follow $P(\nu) \simeq \nu^{-2}$ dependences (where ν is the fluctuation frequency). That may not always be the case (Arthur et al., 1978; Holzworth and Mozer, 1979), and whenever the power is not exactly -2, $D_{\phi\phi}$ (or equivalently D_{LL}) will depend on μ (and possibly J). Westphalen and Spjeldvik (1982) have suggested a method by which the time averaged μ-dependence of $D_{\phi\phi}$ may be deduced from inner zone ($L \sim 1.2$) trapped particle spectra in the keV and lower MeV range, below the energy range where the cosmic ray albedo neutron decay source (CRAND) is important. The actual determination of $D_{\phi\phi}(\mu, J)$ remains to be implemented, however. Detailed investigations of a number of theoretical aspects of the inner edge of the radiation belts have recently been made by Jentsch and Wibberenz (1980) and Jentsch (1981), but are beyond scope of the present review.

Figure 30 shows a comparison of theoretically computed proton, helium and oxygen ion fluxes at $E=0.1-20$ MeV per ion. Notice that in the heart of the radiation belts, $L=3.25$, theory predicts that protons should be the dominant ion species from ~ 100 to $\sim 1{,}000$ keV per ion while helium and oxygen ions should be more numerous when compared at equal total ion energy in the MeV range. The curves are drawn for three different values of the magnetic radial diffusion coefficient, with one fixed electric radial diffusion coefficient, and given observed outer zone boundary conditions; for details see Spjeldvik and Fritz (1978b). Much of the Explorer 45 ion composition data for equatorially mirroring ions support these theoretical results over the limited energy range where the data are available. However, a critical test can only be made when simultaneous proton and heavy ion data are available over a much more extensive energy range. Further studies of the ISEE spacecraft data would be in order.

Comparison of Theory and Observation

Ionic composition observations have been made over two energy ranges, below a few tens of keV and above several hundred keV. Figure 31 (from Williams, 1980) shows the quiet time integral radiation belt particle energy density. It can be seen that the main contribution to the energy density comes from the intermediate energies where our current composition knowledge is lacking. There is much evidence supporting the idea that a substantial fraction of the lower-energy ring current ion population is of ionospheric origin (Lundin et al., 1980; Lennartsson et al., 1981; Lennartsson and Sharp, in press 1982; Williams, 1980; Young et al., 1982), perhaps mixed with solar wind ions, and that the higher energy ions are of extraterrestrial origin (e.g. Hovestadt et al., 1978b). Below ~ 20 keV per ion observations point to H^+, He^+, O^+, O^{++} in variable relative abundances, and above ~ 500 keV per ion the observations reveal ions of hydrogen, helium, carbon, oxygen and heavier ions. The energetic heavy ions are also

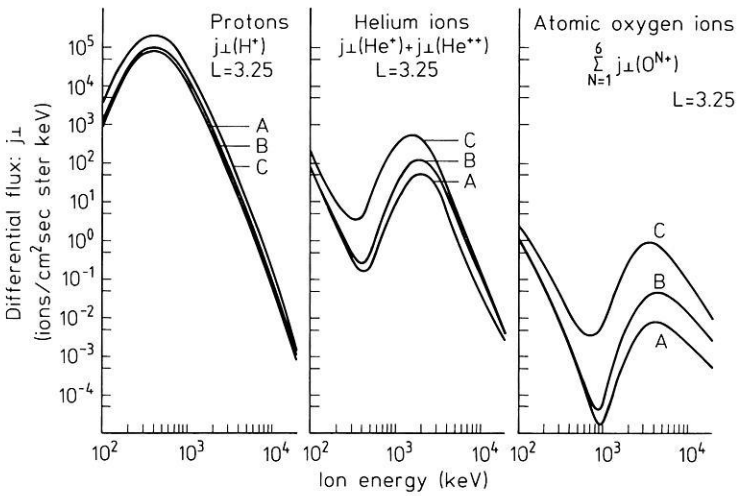

Fig. 30. Theoretical ion composition of the earth's radiation belts. Sensitivity comparison of protons, helium ions, and oxygen ions due to variations in the magnetic diffusive ion transport rate as quantified by the magnetic diffusion coefficient $D_{LL}^{(M)}$. The spectral curves shown for each ion species represent a flux summation over all applicable charge states at an L-shell of 3.25, where the ion fluxes generally maximize in the lower range. The spectral coverage in these panels extends over the energy range 100 keV to 20 MeV per ion. The curves labeled A, B, and C correspond to $D_{LL}^{(M)}$ values of $2 \times 10^{-10} \times L^{10}$, $10^{-9} \times L^{10}$, and $10^{-8} \times L^{10} R_E^2$/day, respectively, with $D_{LL}^{(E)}$ taken as $2 \times 10^{-6} \times L^{10}/(L^4 + (\mu_M/i)^2)\ R_E^2$/day where μ_M is measured in MeV/Gauss and i is the ionic charge state number

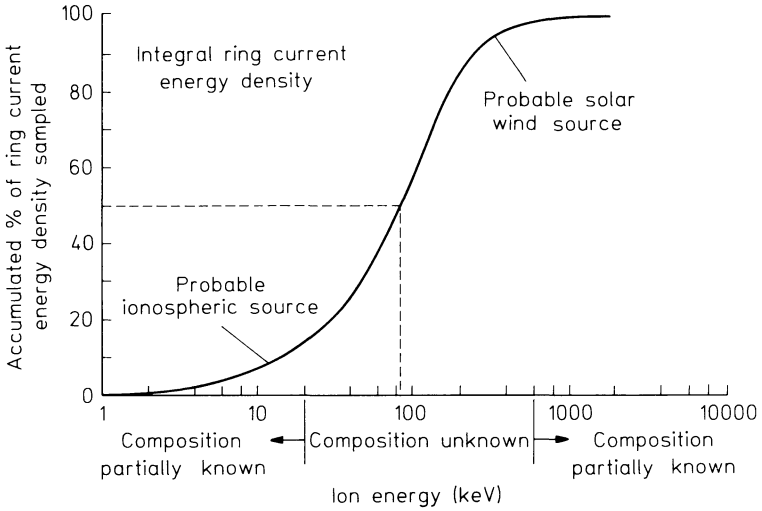

Fig. 31. Integral ring current and radiation belt energy density for quiet time conditions. Indicated are the energy ranges where partial information about the ionic composition is available from experimental data. The contribution to the trapped particle energy density is greatest where this curve is steepest, and that energy range coincides with the energy range where the actual radiation belt composition is unknown

observed to be in the higher charge states (D. Hovestadt, personal communication, 1979).

Unfortunately, most instruments do not permit the determination of the precise ionic charge state distribution. At a given ion energy, the total contribution of a given ion species, $j=\sum_i j_i$, is measured. To compare the theoretically calculated particle distributions with such observations requires the summation of the theoretical results over all ionic charge states. The radiation belt transport and loss relation (1) then yields:

$$\frac{\partial f}{\partial t}=\frac{\partial}{\partial\phi}\left[D_{\phi\phi}\frac{\partial f}{\partial\phi}\right]+\frac{\partial}{\partial z}\left[D_{zz}\frac{\partial f}{\partial z}\right]+\frac{\partial}{\partial J}\left[\left\langle\frac{\Delta J}{\Delta t}\right\rangle f\right]+\frac{\partial}{\partial\mu}\left[\left\langle\frac{\Delta\mu}{\Delta t}\right\rangle f\right]-\Lambda f+S \tag{2}$$

where quantities with no charge state subscript are averaged over all the available ionization states. The ion pitch angle and radial diffusion coefficients become:

$$D_{\phi\phi}=\sum_i D_{\phi\phi_i}\frac{\partial f_i}{\partial\phi}\Big/\sum_i\frac{\partial f_i}{\partial\phi},\qquad D_{zz}=\sum_i D_{zz_i}\frac{\partial f_i}{\partial z}\Big/\sum_i\frac{\partial f_i}{\partial z} \tag{3}$$

while the energy degradation effects on the first and second adiabatic invariants is now described by:

$$\left\langle\frac{\Delta\mu}{\Delta t}\right\rangle=\sum_i\left\langle\frac{\Delta\mu}{\partial t}\right\rangle_i f_i/\sum_i f_i.\qquad\left\langle\frac{\Delta J}{\Delta t}\right\rangle=\sum_i\left\langle\frac{\Delta J}{\partial t}\right\rangle_i f_i/\sum f_i, \tag{4}$$

For the distribution of a given ion species summed over all charge states the charge exchange expressions reduce to a simple weighted loss term where

$$\Lambda=\Lambda_{10}f_1/\sum_i f_i, \tag{5}$$

$$f=\sum_i f_i, \tag{6}$$

and

$$S=\sum_i S_i. \tag{7}$$

As a consequence, one may apply, to the summed distribution function f, an equation similar to that of the distribution function f_i for individual charge states but where the proper coefficients are weighted by the charge state distribution and its derivatives.

In general, the different coefficients vary significantly with the ionic charge state. As an example, the Cornwall (1972) model radial diffusion coefficients D_{LL} (simply related to $D_{\phi\phi}$ by a Jacobian transformation) for electric fluctuations may be written in the form

$$D_{LL_i}^{(E)}=C^{(E)}\frac{L^{10}}{L^4+(\mu_M/i)^2} \tag{8}$$

where the sub-coefficient $C^{(E)}$ depends on the electric field fluctuation magnitude (and has values in the range 2×10^{-6}–2×10^{-5} R_E^2 per day) and μ_M is the magnetic moment in MeV per Gauss. This expression is valid for equatorially mirroring particles; $D_{LL_i}^{(E)}$ and $D_{LL_i}^{(M)}$ vary somewhat with equatorial pitch angle (e.g. Schulz, 1975). At multi-MeV energies the second term in the denominator of (8) dominates and thus $D_{LL_i}^{(E)}\propto i^2$ where i is the ionic charge state number, and in the high energy limit

$$D_{LL}^{(E)}\simeq C^{(E)}L^{10}\mu_M^{-2}\sum_i i^2\frac{\partial f_i}{\partial L}\Big/\sum_i\frac{\partial f_i}{\partial L}. \tag{8}$$

In this limit the ionic charge state distribution is biased towards the higher charge states attainable, and for this reason the effective radial diffusion coefficient may become quite large. A similar situation may exist for ion pitch angle diffusion although the specific details remain to be investigated.

It is also worth noting that the effective rate of ion loss through charge state neutralization (e.g. the process $\underline{O}^+ + H \rightarrow \underline{O} + H^+$; where underlining denotes the energetic particle) scales with the ratio $f_1/\sum_i f_i$. This implies that when $f_1 \ll f_i$ for $i \geqq 2$, the time scale of ion loss due to charge exchange will be very long. Coulomb

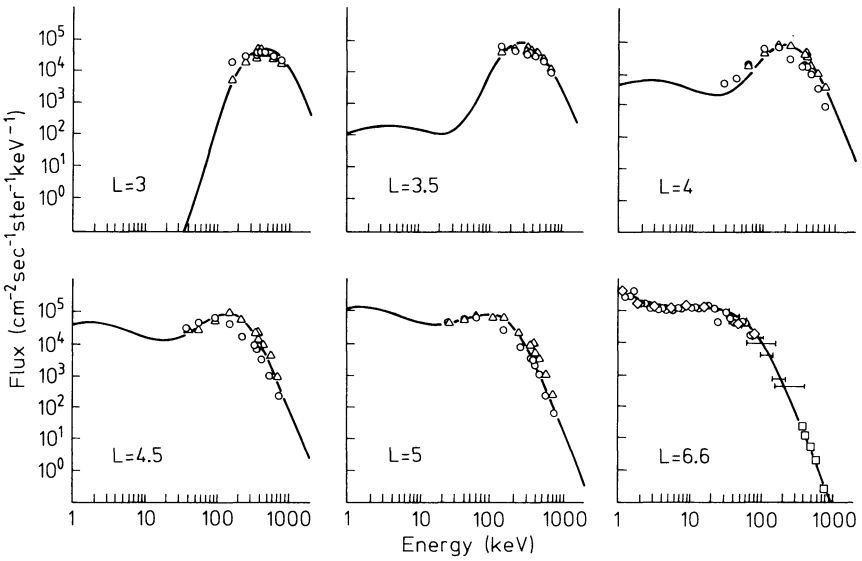

Fig. 32. Radiation belt proton energy spectra; comparison of theoretical and observed energy spectra in the keV energy range at L values of 3, 3.5, 4, 4.5, 5, and 6.6. The spectrum at $L=6.6$ constitutes the adopted boundary condition on the theoretical calculations based on data taken from a number of experiments on the satellite ATS 6 in geostationary orbit (Fritz et al., 1977). The data at the lower L values are taken from quiet time observations on board the satellite Explorer 45. Because an increasing number of detector channels are judged unreliable with decreasing L values, the spectral distribution of valid data is less extensive at the lower L shells (for details, see Spjeldvik, 1977)

collisions, on the other hand, generally have an energy degradation rate following an i^2 dependence (Rossi and Olbert, 1970). Thus, ions in the higher ionic charge states will be degraded in energy at a rate higher than those in the lower charge states; e.g. an O^{6+} ion will have an energy degradation rate 36 times higher than an O^+ ion at the same energy. Consequently, one would expect the spectral shapes of such ions to vary with charge state.

The charge state information for geomagnetically trapped ions cannot be used to infer the ion origin conclusively. Spjeldvik and Fritz (1978b) have demonstrated that charge state altering reactions soon transform the ionic charge state according to internal radiation belt processes. To some limited extent a similar situation might exist for the elemental abundance of trapped ions, since mass dependent processes can change the relative abundances. The latter process is particularly important below a few hundred keV ion energies.

Given suitable boundary conditions in the outer radiation zone, it is possible to compute numerically the radiation belt theoretical distributions of several different ion species. Since these ions are subject to mass and charge dependent interactions with the plasmasphere and exosphere, their relative abundance will result from a combination of source strength and internal radiation belt processes.

Figure 32 shows a direct comparison of proton (ion) observations from Explorer 45 at $L \lesssim 5$ and ATS-6 at $L = 6.6$, and theoretical proton spectra at different L-shells. The outer zone proton fluxes were modeled from the ATS-6 observations so critical comparison can be made only at lower L-shells. Unfortunately, the coverage of uncontaminated Explorer 45 data is substantially less at the lower L-shells, particularly below $L \sim 3$. Nevertheless, the comparison shows a fair agreement, strengthening the idea that the 100–1,000 keV ions are protons. This finding can be further tested by attempting to match the fluxes of another ion species with the proton (ion) data, and this was done by Spjeldvik (1977) who found it difficult to accomplish such a match unless rather extreme assumptions on the rate of radial diffusion together with virtual absence of protons

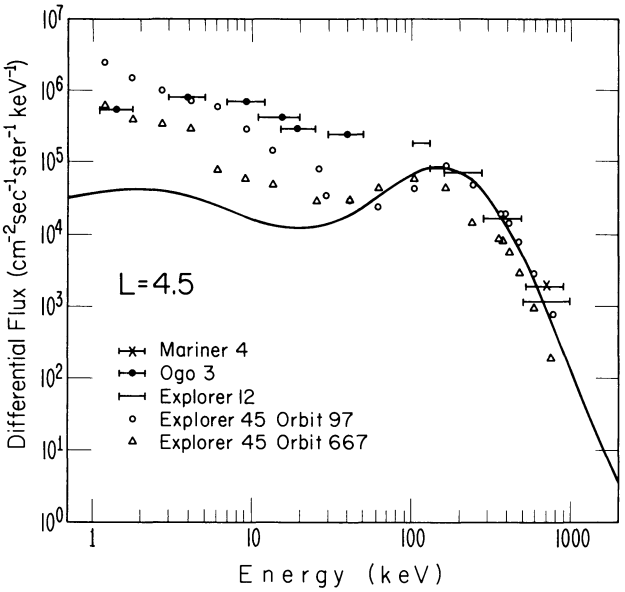

Fig. 33. Comparison between Explorer 45 ion observations at $L=4.5$ and data form OGO 3, Explorer 12, and Mariner 4. Also shown are the theoretically predicted proton fluxes shown as the solid curve. Ion observations at tens of keV may not be protons (see the text). At this L-shell the Explorer 45 data below 40 keV are judged questionable (Spjeldvik, 1977)

were adopted. Thus, the available indirect evidence supports the finding that these ions probably are protons, and to the extent of the valid data from Explorer 45 there is a good agreement between theory and observation at radiation belt energies. There is no agreement at ring current energies ($E < 100$ keV), however. That is depicted in Fig. 33 which compares the theoretical proton spectrum at $L=4.5$ with data from Mariner 4, OGO-3, Explorer 12 and Explorer 45. Presumably some of this discrepancy below ~ 100 keV stems from the possibility that the majority of these ions may not be protons, and some from the effect of non-diffusive transport process operating at these energies.

A similar comparison can also be made for the heavier ions, but only over a short energy range. Figure 34

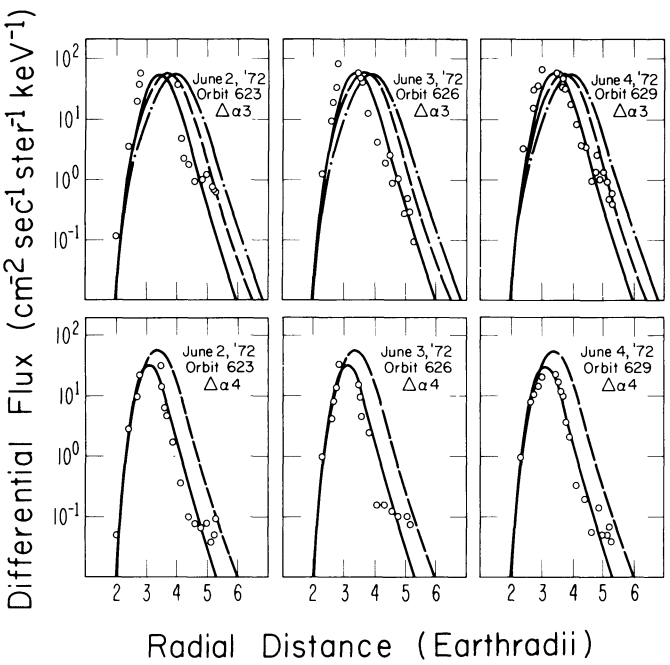

Fig. 34. Radiation belt helium ion radial profiles; comparison between theory and experiment. Circles are observed differential fluxes from the heavy ion experiment on Explorer 45 averaged over the energy passbands $\Delta\alpha 3$ (1.16–1.74 MeV) and $\Delta\alpha 4$ (1.74–3.15 MeV) on three consecutive geomagnetically quiet days, June 2–4, 1972. The lines are theoretical predictions. For the $\Delta\alpha 3$ channels (upper panels) the theoretical curves represent differential fluxes at 2 MeV (solid), 1.5 MeV (dashed and 1.2 MeV (dot-dashed). For the $\Delta\alpha 4$ channels (the lower panels) the theoretical curves represent differential fluxes at 3 MeV (solid) and 2 MeV (dashed) (for details, see Spjeldvik and Fritz, 1978a)

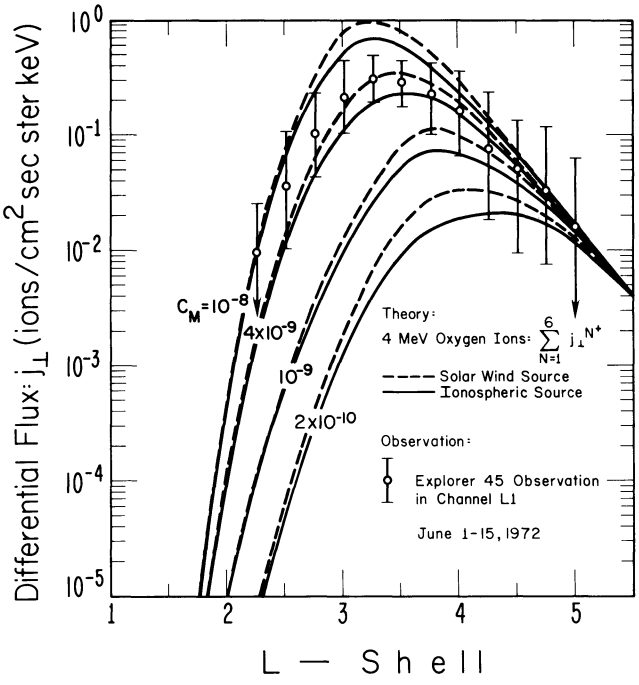

Fig. 35. Radiation belt oxygen ion radial profile; comparison between theory and observation. The lines indicate computed radial profiles of 4 MeV oxygen ions summed over all charge states in the earth's radiation belts. The solid curves assume an ionospheric source of O^+ and the outer zone boundary and show the profiles for $C_M = 2\times10^{-10}$, $C_M = 10^{-9}$, $C_M = 4\times10^{-9}$, and $C_M = 10^{-8} R_E$/day where $D_{LL}^{(M)} = C_M L^{10}$. The dashed curves assume a solar wind source of O^{6+} at the outer zone boundary and show the profiles for the same values of C_M. Data on oxygen ions obtained from the L1 channel on the satellite Explorer 45 are also indicated. The detector passband is 1.82–4.8 MeV per ion for oxygen ions

depicts a comparison of Explorer 45 helium ion observations at 1.16–1.74 and 1.74–3.15 MeV per ion with theoretical results at 1.2, 1.5 and 2, and 2 and 3 MeV per ion respectively. The agreement is quite good for the three quiet days of data used here. A much more critical comparison would be to extend the energy range, particularly towards lower energies where the theory predicts spectral turnover below ~1 MeV. The comparison of oxygen ion theoretical radial distribution and available CNO data is given in Fig. 35, and in spite of the uncertainty in the theoretical curves owing to the input parameter estimates (most notably in the charge exchange cross sections, Spjeldvik and Fritz, 1978b) a fair agreement was achieved. As in the case of helium ions, there is a need for more critical comparison. The data on carbon and oxygen ions now available from the new instruments on ISEE-1 can be used for this purpose when data from suitable spacecraft orbits close to the geomagnetic equatorial plane are selected.

Future Outlook

The last decade has been one of increasing emphasis on precise ionic measurements in the earth's radiation belts. Foremost has been the desire to establish the ion identity and their individual spectral and anisotropy characteristics. Development of fast pulse resolution electronic circuity for spacecruft use has enabled researchers to develop time-of-flight instruments where not only the differential (dE/dx) and total (E) energy deposition of energetic ions incident on solid state detectors could be measured. but also the ionic orbital flight time over a fixed path length within the instrument. Several such instruments have been built and flown. Details of future heavy ion detectors now being developed for the NASA/OPEN mission have been published (Spjeldvik, 1981a; Wilken et al., 1982). Besides three solid state detectors and an ion flight path, such instruments utilize electrostatic deflection of (low energy) secondary electrons emitted by the thin detectors. That eliminates the need for magnets (a weight saving), and microchannel plates provide position sensitive secondary electron measurements. These instruments are expected to provide good mass and energy information from about 200 keV per ion to tens of MeV.

A problem encountered in the in-situ measurements of minor species is related to the often low geometric factor of the instrument. Ions at tens of keV energies can be deflected by a strong electrostatic field (as is commonly done in some mass spectrometer design), and the principle now being invoked is to make the instrument aperture into an annular (ring) shape such that incoming ions are deflected and focused onto a

smaller area detector (D. Bryan and D. Hardy, personal communications, 1980). An instrument now also being developed for the Swedish/VIKING and the NASA/OPEN mission uses this annular (toroidal) aperture geometry (Wilken et al., 1982), and incoming ions are first deflected by a (variable) electric field, then post-accelerated by a known amount and finally detected in a solid state detector. This type of instrument bears the promise of closing the now existing gap in our ability to determine the ion identity at upper ring current energies. Other ion detectors may also be under development, but their current state of design and proprietary considerations preclude a discussion here. Nevertheless, it can be anticipated that the ionic mass and charge composition of the earth's radiation belts will be studied intensively during the coming years.

Acknowledgements. The author has benefitted from many years of collaboration with Dr. Theodore A. Fritz, and from the hospitality of the research division at the NOAA/Space Environment Laboratory in Boulder, Colorado. The work was supported by NASA grants S-50897G and W-14595. Useful discussions with Dr. D. Hovestadt are gratefully acknowledged.

References

Adams, J.H., Partridge, K.: Do trapped heavy ions cause soft upsets on spacecraft? NRL Memorandum Report 4846, Naval Research Laboratory, Washington, D.C., 20375, 1982

Alfven, H., Fälthammar, C.-G.: Cosimal electrodynamics. Oxford, United Kingdom. Clarendon Press 1963

Arthur, C.W., McPherron, R.L., Lanzerotti, L.J., Webb, D.C.: Geomagnetic field fluctuations at synchronous orbit, 1. Power spectra. J. Geophys. Res. **83**, 3859, 1978

Balsiger, H., Eberhardt, P., Geiss, J., Ghielmetti, A., Walker, H.P., Young, D.T., Loidl, H., Rosenbauer, H.: A satellite-borne ion mass spectrometer for the energy range 0 to 16 keV. Space Science Instrumentation **2**, 499, 1976

Bame, S.J., Asbridge, J.R., Feldman, W.C., Montgomery, M.D.: Solar wind heavy ion abundances. Solar Phys. **43**, 463, 1975

Bhonsle, R.V., Degaonkar, S.S., Alurkar, S.K.: Ground-based solar radio observations of the August 1972 events. Space Sci. Rev. **19**, 475, 1976

Blake, J.B., Fennell, J.F., Schulz, M., Paulikas, G.A.: Geomagnetically trapped alpha particles: 2. The inner zone. J. Geophys. Res. **78**, 5498, 1973

Blake, J.B.: Experimental test to determine the origin of geomagnetically trapped radiation. J. Geophys. Res. **78**, 5822, 1973

Blake, J.B.: On the ionic identity of the ring current particles. J. Geophys. Res. **81**, 6189, 1976

Blake, J.B., Fennell, J.F., Hovestadt, D.: Measurements of heavy ions in the low-altitude regions of the outer zone. J. Geophys. Res. **85**, 5992, 1980

Blake, J.B., Fennell, J.F.: Heavy ion measurements in the synchronous altitude region. Planet. Space Sci. **29**, 1205, 1981

Burke, W.J.: An overview of radiation belt dynamics. In: Proceedings of the Air Force Geophysics Laboratory workshop on the Earth's radiation belts: January 26–27, 1981, R.C. Sagalyn, W.N. Spjeldvik and W.J. Burke, eds., pp. 9–46. Air Force Systems Command, AFGL-TR-81-0311, Hanscom AFB, Massachusetts, 1981

Cahill, L.J., Jr.: Response of the magnetosphere during early August 1972, Space Sci. Rev. **19**, 703, 1976

Claflin, E.S.: Charge exchange cross sections for hydrogen and helium ions incident on atomic hydrogen: 1 to 1,000 keV. Report TR-0059 (6260-20)-1, The Aerospace Corporation, El Segundo, California, July 1970

Cornwall, J.M.: Radial diffusion of ionized helium and protons: A probe for magnetospheric dynamics. J. Geophys. Res. **77**, 1756, 1972

Cornwall, J.M., Schulz, M.: Physics of heavy ions in the magnetosphere, In: Solar System Plasma Physics, C.F. Kennell, L.J. Lanzerotti and E.N. Parker, eds. North-Holland Publ. 1979

Davis, L.R., Williamson, J.M.: Low energy trapped protons. Space Sci. Rev. **3**, 365, 1963

Davis, L.R., Williamson, J.M.: Outer zone protons. In: Radiation trapped in the Earth's magnetic field, B.M. McCormac, ed. Dordrecht, Holland: D. Reidel Publ. Co. 1966

Debrunner, H., Lockwood, J.A.: The spatial anisotropy, rigidity spectrum and propagation characteristics of the relativistic solar particles during the event on May 7, 1978. J. Geophys. Res. **85**, 6853, 1980

Fälthammer, C.-G.: Radial diffusion by violation of the third adiabatic invariant. In: Earth's particles and fields, Ed.: B.M. McCormac, ed.: p. 157. New York: Reinhold Publishing 1968

Fennell, J.F., Blake, J.B., Paulikas, G.A.: Geomagnetically trapped alpha particles: 3. Low-altitude alpha-proton comparisons. J. Geophys. Res. **79**, 521, 1974

Fennell, J.F., Blake, J.B.: Geomagnetically trapped alpha particles. In: Magnetospheric particles and fields, B.M. McCormac, ed.: p. 149. Dordrecht, Holland: D. Reidel Publ. Co. 1976

Fritz, T.A., Williams, D.J.: Initial observations of geomagnetically trapped alpha particles at the equator. J. Geophys. Res. **78**, 4719, 1973

Fritz, T.A., Cessna, J.R.: ATS-6 NOAA low energy proton experiment. IEEE, transactions on aerospace and electronic systems, **AES-11**, 1145, 1975

Fritz, T.A.: Ion Composition. In: Physics of the Solar planetary environments, D.J. Williams, ed.: p. 716. Washington, D.C.: American Geophys. Union 1976

Fritz, T.A., Wilken, B.: Substorm generated fluxes of heavy ions at the geostationary orbit. In: Magnetospheric particles and fields, B.M. McCormac, ed.: p. 171. Dordrecht, Holland: D. Reidel Publ. Co. 1976

Fritz, T.A., Arthur, C.W., Coleman, P.J., Jr., Cummings, W.D., DeForest, S.E., Erickson, K.N., Konradi, A., Masley, A.J., Mauk, B.H., McIlwain, C.E., McPherron, R.L., Paulikas, G.A., Pfitzer, K.A., Reasoner, D.L., Satterblom, P.R., Su, S.Y., Walker, R.J., Whipple, E.C., Jr., Winckler, T.R.: Significant Initial Results from ATS-6. NASA Technical Paper 1101, Goddard Space Flight Center, Maryland, 1977

Fritz, T.A., Spjeldvik, W.N.: Observations of energetic radiation belt helium ions at the geomagnetic equator during quiet conditions. J. Geophys. Res. **83**, 2579, 1978

Fritz, T.A.: The S^3 solid state proton detector experiment. Technical Memorandum, NOAA, U.S. Dept. of Commerce, Washington, D.C., 1979

Fritz, T.A., Spjeldvik, W.N.: Simultaneous quiet time observations of energetic radiation belt protons and helium ions: The equatorial α/ρ-ratio near 1 MeV. J. Geophys. Res. **84**, 2608, 1979

Fritz, T.A., Spjeldvik, W.N.: Pitch angle distributions of geomagnetically trapped MeV helium ions during quiet times. J. Geophys. Res. **87**, 5095, 1982

Gosling, J.T., Asbridge, J.R., Bame, S.J., Feldman, W.C., Paschmann, G., Sckopke, N.: Solar wind ions accelerated to 40 keV by shock wave disturbances. J. Geophys. Res. **85**, 744, 1980

Hakura, Y.: Interdisciplinary summary of solar/interplanetary events during August 1972. Space Sci. Rev. **19**, 411, 1976

Hamilton, D.C., Gloeckler, G., Krimigis, S.M., Bostrom, C.O.,

Armstrong, T.P., Axford, W.I., Fan, C.Y., Lanzerotti, L.J., Hunten, D.M.: Detection of energetic hydrogen molecules in Jupiter's magnetosphere by Voyager 2: Evidence for an ionospheric plasma source. Geophys. Res. Lett. **7**, 813, 1980

Hamlin, D.A., Karplus, R., Vik, R.C., Watson, K.M.: Mirror and azimuthal drift frequencies for geomagnetically trapped particles. J. Geophys. Res. **66**, 1, 1961

Hess, W.N.: The radiation belt and magnetosphere. Waltham, Massachusetts: Blaisdell Publishing Co. 1968

Hirshberg, J.: Helium abundance in the sun. Rev. Geophys. Space Phys. **11**, 115, 1973

Hirshberg, J.: Composition of the solar wind: Present and past. Rev. Geophys. Space Phys. **13**, 1059, 1975

Hoffman, R.A., Cahill, L.J., Jr., Anderson, R.R., Maynard, N.C., Smith, P.H., Fritz, T.A., Williams, D.J., Konradi, A., Gurnett, D.A.: Explorer 45 (S^3-A) observations of the magnetosphere and magnetopause during the August 4-6, 1972 magnetic storm period. J. Geophys. Res. **80**, 4287, 1975

Holzworth, R.H., Mozer, S.F.: Direct evaluation of the radial diffusion coefficient near $L=6$ due to electric field fluctuations. J. Geophys. Res. **84**, 2559, 1979

Hovestadt, D., Vollmer, O.: A satellite experiment for detecting low energy heavy cosmic rays. Proceedings of the 12th International Conference on Cosmic Rays **4**, 1608, 1971

Hovestadt, D., Häusler, B., Scholer, M.: Observations of energetic particles at very low altitudes near the geomagnetic equator. Phys. Rev. Lett. **28**, 1340, 1972a

Hovestadt, D.E., Achtermann, E., Ebel, B., Hausler, B., Paschmann, G.: New observations of the proton population of the radiation belt between 1.5 and 104 MeV. In: Earth's magnetospheric processes, B.M. McCormac, ed.: p. 115. Dordrecht, Holland: D. Reidel Publ. Co. 1972b

Hovestadt, D., Gloecker, G., Fan, C.Y., Fisk, L.A., Ipavich, F.M., Klecker, B., O'Gallagher, J.J., Scholer, M., Arbinger, H., Cain, J., Hofner, H., Kunneth, E., Laeverenz, P., Tums, E.: The nuclear and ionic charge distribution particle experiments on the ISEE-1 and ISEE-C spacecraft. IEEE, Transactions Geoscience Electronics **GE16,** 166, 1978a

Hovestadt, D., Gloeckler, G., Fan, C.Y., Fisk, L.A., Ipavich, F.M., Klecker, B., O'Gallagher, J.J., Scheler, M.: Evidence for solar wind origin of energetic heavy ions in the Earth's radiation belt. Geophys. Res. Lett. **5**, 1055, 1978b

Hovestadt, D., Klecker, B., Mitchell, E., Fennell, J.F., Gloeckler, G., Fan, C.Y.: Spatial distribution of $Z \geqq 2$ ions in the outer radiation belt during quiet conditions. Adv. Space Res. **1**, 305, 1981

Intriligator, D.S.: The August 1972 solar-terrestrial events: Solar wind plasma observations. Space Sci. Rev. **19**, 629, 1976

Ivanova, T.A., Maslov, V.D., Panasyuk, M.I., Sosnovets, E.N.: Radiation measurements on the Cosmos-900 Satellite: 3. Spectrometry of protons and Alpha-particles with energies greater than 1 MeV/nucleon. Kosmicheskie Issledovaniya **18**, 567 1980

Jentsch, V., Wibberenz, G.: An analytic study of the energy and pitch angle distribution of inner-zone protons. J. Geophys. Res. **85**, 1, 1980

Jentsch, V.: On the role of external and internal source in generating energy and pitch angle distributions of inner-zone protons. J. Geophys. Res. **86**, 701, 1981

Johnson, R.G., Sharp, R.D., Shelley, E.G.: The discovery of energetic He^+ ions in the magnetosphere. J. Geophys. Res. **79**, 3135, 1974

Johnson, R.G., Sharp, R.D., Shelley, E.G.: Composition of the hot plasmas in the magnetosphere. In: Physics of the Hot Plasma in the Magnetosphere, B. Hultqvist and L. Stenflo, eds: p. 45. New York: Plenum Publ. Co. 1975

Johnson, R.G., Sharp, R.D., Shelley, E.G.: Observations of the ring current composition during the 29 July 1977 magnetic storm. EOS, Trans. Am. Geophys. Union **58**, 1217, 1977

Johnson, R.G., Sharp, R.D., Shelley, E.G.: Observations of ions of ionospheric origin in the storm-time ring current. Geophys. Res. Lett. **5**, 59, 1978

Johnson, R.G.: Energetic ion composition in the Earth's magnetosphere. U.S. National Report to the IUGG, David E. James, ed. Rev. Geophys. Space Phys. **17**, 696, 1979

Jordan, C.: The ionization equilibrium of elements between carbon and nickel, Monthly Not. R. Astron. Soc. **142**, 501, 1969

Joselyn, J.A., Lyons, L.R.: Ion cyclotron wave growth calculated from satellite observations of the proton ring current during storm recovery. J. Geophys. Res. **81**, 2275, 1976

Krimigis, S.M., Van Allen, J.A.: Geomagnetically trapped alpha particles. J. Geophys. Res. **72**, 5779, 1967

Krimigis, S.M., Verzariu, P., Van Allen, J.A., Armstrong, T.P., Fritz, T.A., Randall, B.A.: Trapped energetic nucleii $Z \geqq 3$ in the Earth's outer radiation zone. J. Geophys. Res. **75**, 4210, 1970

Lanzerotti, L.J., MacLennan, C.G.: Solar particle observations during the August 1972 event. In: Correlated interplanetary and magnetospheric observations, D.E. Page, ed.: p. 587, Dordrecht-Holland, D. Reidel Publ. Co. 1974

Lennartsson, W., Sharp, R.D., Shelley, E.G., Johnson, R.G., Balsiger, H.: Ion composition and energy distribution during 10 magnetic storms. J. Geophys. Res. **86**, 4628, 1981

Lennartsson, W., Sharp, R.D.: A comparison of the near equatorial ion composition between quiet and disturbed conditions. J. Geophys. Res., in press 1982

Lundin, R., Lyons, L.R., Pissarenko, N.: Observations of the ring current composition at L-values less than 4. Geophys. Res. Lett. **7**, 425, 1980

Lyons, L.R., Thorne, R.M., Kennel, C.F.: Electron pitch angle diffusion driven by oblique Whistler-mode turbulence. J. Plasma Phys. **6**, 589, 1971

Lyons, L.R., Thorne, R.M., Kennel, C.F.: Pitch angle diffusion of radiation belt electrons within the plasmasphere. J. Geophys. Res. **77**, 3455, 1972

Lyons, L.R., Thorne, R.M.: Equilibrium structure of radiation belt electrons. J. Geophys. Res. **78**, 2142, 1973

Lyons, L.R., Williams, D.J.: The storm and poststorm evolution of energetic (35-560 keV) radiation belt electron distributions. J. Geophys. Res. **28**, 3985, 1975

Lyons, L.R., Williams, D.J.: Storm-associated variations of equatorially mirroring ring current protons, 1-800 keV, at constant first adiabatic invariant. J. Geophys. Res. **81**, 216, 1976

Lyons, L.R.: Plasma Processes in the Earth's radiation belts. In: Solar System plasma physics, C.F. Kennel, L.J. Lanzerotti and E.N. Parker, eds. North-Holland Publ. Co. 1979

Lyons, L.R., Williams, D.J.: A source for the geomagnetic storm main phase ring current. J. Geophys. Res. **85**, 523, 1980

Lyons, L.R., Moore, T.E.: Effects of charge exchange on the distribution of ionospheric ions trapped in the radiation belts near synchronous orbit. J. Geophys. Res. **86**, 5885, 1981

Malitson, H.H., Fainberg, H.H., Stone, R.G.: Hectometric and kilometric solar radio emission observed from satellites in August 1972. Space Sci. Rev. **19**, 511, 1976

Ma Sung, L.S., Gloeckler, G., Fan, C.Y., Hovestadt, D.: Observations of the mean ionization states of energetic particles in the vicinity of the Earth's magnetosphere. J. Geophys. Res. **85**, 5983, 1980

Matsushita, S.: Ionospheric and thermospheric responses during August 1972 storm — A review. Space Sci. Rev. **19**, 713, 1976

McNulty, P.J.: Radiation effects on electronic systems. In: Proceedings of the Air Force Geophysics Laboratory workshop on the Earth's radiation belts: January 26-27,

1981, R.C. Sagalyn, W.N. Spjeldvik and W.J. Burke, eds.: pp. 99–124. Air Force Systems Command, AFGL-TR-81-0311, Hanscom AFB, Massachusetts, 1981
Miller, F.D.: Solar-cometary relations and the events of June-August 1972. Space Sci. Rev. **19**, 739, 1976
Mogro-Campero, A.: Geomagnetically trapped carbon, nitrogen and oxygen nucleii. J. Geophys. Res. 77, 2799, 1972
Nakada, N.P., Mead, G.D.: Diffusion of protons in the outer radiation belt, J. Geophys. Res. **70**, 4777, 1965
Nakagawa, Y.: Flares of August 1972: Analysis of dynamics. Space Sci. Rev. **19**, 459, 1976
Panasyuk, M.I., Reizman, S.Ya., Sosnovets, E.N., Filatov, V.N.: Experimental results of proton and alpha-particle measurements at energies more than 1 MeV/nucleon in the radiation belts. Geomagn. Aeron. **15**, 887, 1977
Panasyuk, M.I., Sosnovets, E.N.: Radiation measurements on the Cosmos-900 satellite: 3. Spectrometry of protons and alpha-particles with energies greater than 1 MeV/nucleon. Kosmicheskie Issledovaniya **18**, 567, 1980
Panasyuk, M.I.: Charge state of energetic ions, (in Russian). Kosmicheskie Issledovaniya **18**, 83, 1980. English translation in: Cosmic Research, **18**, 64, 1980
Panasyuk, M.I., Vlasova, N.A.: Anisotropy of fluxes of protons and alpha particles with energies greater than 4 MeV in the radiation belts. Cosmic Research, **19**, 52, 1981
Pesses, M.E., Tsurutani, B.T., Van Allen, J.A., Smith, E.J.: Acceleration of energetic protons by interplanetary shocks. J. Geophys. Res. **84**, 7297, 1979
Randall, B.A.: Time variation of magnetospheric intensities of outer zone protons, alpha particles and ions ($Z>2$). University of Iowa, Report 73-3, 1973
Rao, U.R.: High energy cosmic ray observations during August 1972 Space Sci. Rev. **19**, 533, 1976
Reagan, J.B., Meyerott, R.E., Nightingale, R.W., Gunton, R.C., Johnson, R.G., Evans, J.E., Imhof, W.L., Heath, D.F., Krueger, A.J.: Effects of the August 1972 solar particle events on stratospheric ozone. J. Geophys. Res **86**, 1473, 1981
Roederer, J.G.: Dynamics of geomagnetically trapped radiation. New York: Springer-Verlag 1970
Rossi, B., Olbert, S.: Introduction to the physics of space. New York: McGraw-Hill 1970
Scholer, M., Ipavich, F.M., Gloekler, G., Hoverstadt, D.: Conditions for acceleration of energetic ions $\gtrsim 30$ keV associated with the Earth's bow shock. J. Geophys. Res. **85**, 4602, 1980
Schulz, M., Lanzerotti, L.J.: Particle diffusion in the radiation belt. New York: Springer-Verlag 1974
Schulz, M.: Geomagnetically trapped radiation. Space Sci. Rev. **17**, 481, 1975
Schulz, M.: Pitch angle diffusion in canonical coordinates: A theoretical formulation. Astrophys. Space Sci., in press 1981
Sharp, R.D., Johnson, R.G., Shelley, E.G., Harris, K.K.: Energetic O^+ ions in the magnetosphere. J. Geophys. Res. **79**, 1844, 1974a
Sharp, R.D., Johnson, R.G., Shelley, E.G.: Satellite measurements of auroral alpha particles. J. Geophys. Res. **79**, 5167, 1974b
Sharp, R.D., Johnson, R.G., Shelley, E.G.: The morphology of energetic O^+ ions during two magnetic storms: Temporal variations. J. Geophys. Res. **81**, 3283, 1976a
Sharp, R.D., Johnson, R.G., Shelley, E.G.: The morphology of energetic O^+ ions during two magnetic storms: Latitudinal variations. J. Geophys. Res. **81**, 3292, 1976b
Sharp, R.D., Shelley, E.G., Johnson, R.G.: A search for helium ions in the recovery phase of a magnetic storm. J. Geophys. Res. **82**, 2361, 1977a
Sharp, R.D., Johnson, R.G., Shelley, E.G.: Observation of an ionospheric acceleration mechanism producing energetic (keV) ions primarily normal to the geomagnetic field direction. J. Geophys. Res. **82**, 3324, 1977b
Shelley, E.G., Johnson, R.G., Sharp, R.D.: Satellite observations of energetic heavy ions during a geomagnetic storm. J. Geophys. Res. **77**, 6104, 1972
Shelley, E.G., Johnson, R.G., Sharp, R.D.: Morphology of energetic O^+ in the magnetosphere. In: Magnetospheric physics, B.M. McCormac, ed.: pp. 135–139. Dordrecht, Holland: D. Reidel Publ. Co. 1974
Shelley, E.G., Sharp, R.D., Johnson, R.G.: Satellite observations of an ionospheric acceleration mechanism. Geophys. Res. Lett. **3**, 654, 1976a
Shelley, E.G., Sharp, R.D., Johnson, R.G.: He^{++} and H^+ flux measurements in the dayside cusp: Estimates of convection electric field. J. Geophys. Res. **81**, 2363, 1976b
Shelley, E.G., Sharp, R.D., Johnson, R.G.: Ion composition in the quiet time magnetosphere. EOS, Trans. Am. Geophys. Union **58**, 1217, 1977
Shelley, E.G.: Heavy ions in the magnetosphere. Space Sci. Rev. **23**, 465, 1979
Simnett, G.M.: Solar cosmic radiation during August 1972. Space Sci. Rev. **19**, 579, 1976
Smith, E.J.: The August 1972 solar-terrestrial events: Interplanetary magnetic field observations. Space Sci. Rev. **19**, 661, 1976
Söraas, F., Davis, L.R.: Temporal variations of the 100 keV to 1,700 keV trapped protons observed on satellite Explorer 26 during the first half of 1965. NASA/Goddard Space Flight Center, Report X-612-68-328, Maryland, 1968
Spjeldvik, W.N., Thorne, R.M.: The cause of storm after effects in the middle latitude D-region. J. Atmos. Terr. Phys. **37**, 777, 1975
Spjeldvik, W.N.: Equilibrium structure of equatorially mirroring radiation belt protons. J. Geophys. Res. **82**, 2801, 1977
Spjeldvik, W.N., Fritz, T.A.: Energetic ionized helium in the quiet time radiation belts: Theory and comparison with observation. J. Geophys. Res. **83**, 654, 1978a
Spjeldvik, W.N., Fritz, T.A.: Theory for charge states of energetic oxygen ions in the Earth's radiation belts. J. Geophys. Res. **83**, 1583, 1978b
Spjeldvik, W.N., Fritz, T.A.: Composition of the hot plasma in the inner magnetosphere: Observations and theoretical analysis of protons, helium ions and oxygen ions. Space Research, **XVIII**, 317, 1978c
Spjeldvik, W.N., Fritz, T.A.: Quiet time observations of equatorially trapped megaelectronvolt radiation belt ions with nuclear charge $Z \geqq 4$. *J. Geophys. Res.* **83**, 4401, 1978d
Spjeldvik, W.N.: Expected charge states of energetic ions in the magnetosphere. Space Sci. Rev. **23**, 499, 1979
Spjeldvik, W.N.: State of the art of energetic particle measurements in the Earth's magnetosphere. In: Proceedings of the Air Force Geophysics Laboratory workshop on the Earth's radiation belt: January 26–27, 1981, R.C. Sagalyn, W.N. Spjeldvik and W.J. Burke eds.: pp. 125–208. Air Force Systems Command, AFGL-TR-81-0311, Hanscom AFB, Mass., 1981a
Spjeldvik, W.N.: Modelling of magnetically trapped radiation in the inner magnetosphere of the Earth. In: Proceedings of the Air Force Geophysics Laboratory workshop on the Earth's radiation belts: January 26–27, 1981 R.C. Sagalyn, W.N. Spjeldvik and W.J. Burke, eds.: pp. 245–270. Air Force Systems Command, AFGL-TR-81-0311, Hanscom AFB, Mass., 1981b
Spjeldvik, W.N., Fritz, T.A.: Observations of energetic helium ions in the Earth's radiation belts during a sequence of geomagnetic storms. J. Geophys. Res. **86**, 2317, 1981a
Spjeldvik, W.N., Fritz, T.A.: Energetic heavy ions with nuclear charge $Z \geqq 4$ in the equatorial radiation belts of the Earth: Magnetic storms. J. Geophys. Res. **86**, 2349 1981b
Spjeldvik, W.N., Fritz, T.A.: Observations of ions with nucle-

ar charge $Z \geqq 9$ in the inner magnetosphere. J. Geophys. Res. **86**, 7749, 1981c
Spjeldvik, W.N., Fritz, T.A.: Experimental determination of geomagnetically trapped energetic heavy ion fluxes. In: Energetic ion composition of the Earth's magnetosphere, Advances in Earth and Planet. Sci., **5**, R.G. Johnson, ed. Tokyo: Terra Scientific Publishing, in press 1982.
Störmer, C.: The Polar Aurora. Oxford: Clarendon Press 1955
Tinsley, B.A.: Evidence that the recovery phase ring current consists of helium ions. J. Geophys. Res. **81**, 6193, 1976
Vaisberg, O.L., Zastenker, G.N.: Solar wind and magnetosheath observations at earth during August 1972. Space Sci. Rev. **19**, 687, 1976
Van Allen, J.A., Randall, B.A., Krimigis, S.M.: Energetic C, N, O nuclei in the Earth's outer radiation zone. J. Geophys. Res. **75**, 6085, 1970
Webber, W.R., Roelof, E.C., McDonald, F.B., Teegarden, B.J., Trainor, J.: Pioneer 10 measurements of the charge and energy spectrum of solar cosmic rays during 1972 August. Astrophys. J. **199**, 482, 1975
West, H.I., Jr., Buck, R.M., Walton, J.R.: Electron pitch angle distributions throughout the magnetosphere as observed with OGO-5. J. Geophys. Res. **78**, 1064, 1973
West, H.I., Jr., Buck, R.M., Davidson, G.: Study of energetic electrons in the outer radiation belt regions using data obtained by the LLL spectrometer on OGO-5 in 1968. Lawrence Livermore Laboratory Report **UCRL-52807,** California, 1979
West, H.I., Jr., Buck, R.M., Davidson, G.T.: The dynamics of energetic electrons in the Earth's outer radiation belt during 1968 as observed by the Lawrence Livermore National Laboratory's spectrometer on OGO-5. J. Geophys. Res. **86**, 2111, 1981
Westphalen, H., Spjeldvik, W.N.: On the energy dependence of the radial diffusion coefficient and spectra of inner radiation belt particles: Analytic solutions and comparison with numerical results. J. Geophys. Res. **87**, 8321, 1982
Wilken, B., Fritz, T.A., Stüdemann, W.: Experimental techniques for ion composition measurements in space. Nuclear Instruments and Methods **196**, 161, 1982
Williams, D.J., Lyons, L.R.: The proton ring current and its interaction with the plasmapause: Storm recovery phase. J. Geophys. Res. **79**, 4195, 1974a
Williams, D.J., Lyons, L.R.: Further aspects of the proton ring current interaction with the plasmapause: Main and recovery phases. J. Geophys. Res. **79**, 4791, 1974b
Williams, D.J., Keppler, E., Fritz, T.A., Wilken, B., Wibberenz, G.: The ISEE 1 and 2 medium energy particle experiment. IEEE, Transactions on Geoscience Electrons **GE-16,** 270, 1978
Williams, D.J.: Ring current composition and sources. In: Dynamics of the magnetosphere, S.I. Akasofu, ed.: pp. 407–424. Dordrecht, Holland: D. Reidel Publ. Co. 1980
Williams, D.J.: Ring current composition and sources: An update. Planet. Space Sci. **29**, 1195, 1981
Williams, D.J.: The Earth's ring current: Causes , generation and decay. Space Sci. Rev., in press 1982
Young, D.T., Balsiger, H., Geiss, J.: Correlations of magnetospheric ion composition with geomagnetic and solar activity. J. Geophys. Res., in press 1982
Young, D.T., Ion composition and dynamics at ring current energies. J. Geophys. (this issue), 1983

Received November 12, 1982; Revised version February 10, 1983
Accepted February 10, 1983